Origin and evolution of groundwater in the Goharzamin mine area using hydro-geochemical and isotopic analyses

Amir Saberinasr

a.saberinasr@scu.ac.ir

Shahid Chamran University of Ahvaz https://orcid.org/0000-0001-7705-0004

Nasrollah Kalantari

Shahid Chamran University of Ahvaz

Hassan Ghelichpour

Goharzamin mining and industrial company

Massoud Morsali

University of Isfahan

Research Article

Keywords: Radiocarbon dating, Mine Seepages, hydrochemical interpretations, saline water

Posted Date: August 9th, 2024

DOI: https://doi.org/10.21203/rs.3.rs-4064449/v1

Version of Record: A version of this preprint was published at Mine Water and the Environment on February 20th, 2025. See the published version at https://doi.org/10.1007/s10230-025-01032-5.

Origin and evolution of groundwater in the Goharzamin mine area using hydro-geochemical and isotopic analyses

Amir Saberinasr[1], Nasrollah Kalantari[2], Hassan Ghelichpour[3], Massoud Morsali[4]

[1]*Department of Geology, Faculty of Earth sciences, Shahid Chamran University of Ahvaz, Ahvaz, Iran, a.saberinasr@scu.ac.ir, ORCID 0000-0001-7705-0004*

[2]*Department of Geology, Faculty of Earth sciences, Shahid Chamran University of Ahvaz, Ahvaz, Iran, n.kalantari@scu.ac.ir, ORCID 0000-0001-7657-8229*

[3]*Geological Department Head of Goharzamin Mining and Industrial Company, Kerman, Iran, hassanghlichpor@yahoo.com*

[4]*Department of Geology, University of Isfahan, Isfahan, Iran, m.morsali@sci.ui.ac.ir, ORCID 0000-0002-2211-0951*

Abstract

Determining the source of groundwater infiltrating mine pits is one of the most interesting challenge for mining engineers and designers. The uncontrolled groundwater flow will delay the planned schedule and have a negative impact on extraction costs and mining operations. Determining the groundwater source by hydrochemical and isotopical interpretations in the Goharzamin iron mine, located in south-central Iran, plays a significant role in comprehending hydrochemical and hydrogeological processes and designing an effective dewatering system in this mining area. Through three phases of groundwater sample collection from seepages and boreholes, a total of 75 samples were gathered for analysis, including 12 samples containing heavy metals and stable isotopic data (D and ^{18}O), 5 samples containing ^{14}C and ^{13}C, and another 5 samples containing ^{3}H data. Results indicated that all samples belonged to saline and brackish water categories (EC > 4 mS cm^{-1}), with a predominant sequence of Cl^{-}-SO_4^{2-}-HCO_3^{-}-NO_3^{-}, and Na^{+}-Ca^{2+}-Mg^{2+}-K^{+} for anions and cations, respectively. Conservative tracers (Cl, Br, and B) and stable isotopes demonstrated that Kheirabad Salt Lake (located approximately 13 km north of the mine) is unlikely to be the source of groundwater. Radiocarbon and tritium age dating suggested that the majority of groundwater in the mining area was infiltrated during the Holocene and late Pleistocene epochs (paleowater) rather than being replenished by recent rainfall. Hydrochemical variations observed in samples collected during the wet season are generally attributed to the mixing of surface water and groundwater at fractures around the mine pit.

Keywords Radiocarbon dating, Mine Seepages, hydrochemical interpretations, saline water.

Introduction

Groundwater flow and its negative effects should be considered during mining operations. When mining is performed below the groundwater level, especially in large and deep open-pit mines, water infiltrates into the mine pit from the surrounding formations and geological features, such as fault zones, wall cracks, open fractures, and dykes. This may cause a significant drawdown in groundwater levels, locally or regionally. Groundwater drawdown results in the expansion of the depression cone, leading to changes in groundwater flow and, an increase in groundwater flow and the transport of solutes around the mine. This phenomenon has a significant impact on both the quantity and quality of the mine seepage waters. These are important factors in determining the mining schedule and result in a general increase in mining costs. In mining operations, dry working conditions are preferred due to their ability to reduce the degradation of machinery and tires, consequently decreasing earth-moving costs. Preventing water from entering the mine pit increases safety, ensuring that mining operations can be carried out efficiently and effectively (Surinaidu et al. 2014; Wu et al. 2017; Li et al. 2021). To mitigate the risks associated with groundwater intrusion into the mine pit, several methods, such as diversion, dewatering, sealing, or a combination

thereof, can be implemented. It is crucial to determine the origin of groundwater seepages in order to select the most cost-effective and suitable technique.
Groundwater chemical composition involves the spatial and temporal variations due to precipitation, water-rock interaction, evaporation, redox reactions, recharge water quality, reactions of ion exchange, sorption, dissolution, climate, the grade of chemical weathering of different types of rock, mixing processes, etc. Hydrogeochemical analysis techniques in combination with stable isotope analysis (e.g., ^{18}O and ^{2}H), radioisotopes (e.g., ^{3}H and ^{14}C), and statistical techniques (e.g., Principal-Component-Analysis (PCA) and Hierarchical-Cluster-Analysis (HCA)) are often applied as effective methods to provide significant information regarding similarities among groundwater samples and/or hydrochemical variables, the groundwater residence times in aquifers, the source of groundwater in reservoirs, the groundwater movement's rate and direction, hydrochemical reactions in aquifers, climatic conditions during the recharge, hydraulic connection between different water sources, geological structure of aquifers, and anthropogenic impacts on aquifers (Zouari et al. 2011; Fang 2019; Acikel and Ekmekci 2021; Okofo et al. 2022; Zhao et al. 2022; Nayak et al. 2023; Ju et al. 2024; Hamma et al. 2024; amongst many others). These analysis techniques play a crucial role in enhancing our comprehension of hydrogeological systems.

Goharzamin is an important open-pit iron mine located in the south of Kerman, Iran. The mine has been operating for about 15 years. As the bottom of the pit is around 120 meters below the groundwater level, the groundwater infiltrates the walls and floor. Because pit excavation is a relatively new activity, there have been limited hydrogeological studies undertaken in the area. In recent years, the water seepage problem has led to an effort to design a dewatering network. As a result, efforts have been made to determine the hydrochemical properties of groundwater seepages that fall into the Goharzamin mine pit and find the source of them. The research conducted by Jahanshahi and Zare (2017) has identified Khairabad Playa, located in the north of the Goharzamin pit (about 13 km), as the primary source of salinity. They attributed this to the excavation of the pit, which changed the hydrological conditions of the area. In other words, the playa could account for the brine groundwater's presence. Heidarinejad et al. (2017) identified two hydraulically connected rocky and alluvial aquifers that are probably not associated with the playa. Assari (2019), based on simple hydrochemistry and geological evidences revealed that there are a minimum of three aquifers (two alluvial aquifers and one hard-rock aquifer). Furthermore, Gharaat et al. (2022) demonstrated that the area is comprised of three distinct aquifers: the upper alluvial aquifer, the lower alluvial aquifer, and the hardrock aquifer. The chemical and isotopic findings further verified the distinct source and age of the groundwater. In addition to the aforementioned studies, 11 exploration boreholes encountered a groundwater artesian zone (confined aquifer) in the hard rocks of the area, and their boring was ceased. The groundwater samples exhibited an electrical conductivity (EC) of as high as several mS cm^{-1} (> 50 mS cm^{-1}) that took place in the range of brine (saline and/or hypersaline) groundwater. As a result, this study aims to reassess the age and origin of the waters by employing different analyses and samples, a combination of statistical, hydrochemical, and isotopic studies, and applying diverse interpretations and charts to address the inconsistencies and ambiguities in previous research. Finding the groundwater source and the variables affecting the chemical composition of water will greatly help in designing the mine's dewatering network.

Study Area

Location and meteorologic conditions

The Gol-E-Gohar 3 (Goharzamin) iron mine is situated in the southwestern part of Iran's Kerman province, extending from 29° 5' E to 29° 7' E longitude and 55° 16' N to 55° 18' N latitude, along planar desert topography (Fig. 1). The average elevation of the region exceeds 1700 m above sea level (asl). In this area, Goharzamin (pit No. 3) is the most important mining pit, with a dimension of approximately 1300×1700 m and a deposit of around 640 megatons. The climate of the mining area exhibits a warm temperate and semiarid nature, which is often affected by the Mediterranean pluviseasonal-continental climate. Extended dry seasons characterize the region (7–9 months/year), and the rainfall's seasonal distribution

demonstrates that more than 90% of the annual precipitation concentrated in the winter and early spring seasons, from January to May. The average annual precipitation and temperature stand at less than 150 mm $year^{-1}$ and approximately 18.5°C, respectively. The potential evaporation rate is higher than the precipitation rate for a significant portion of the year. Monthly temperatures vary between 6.5°C (in January) and 30°C (in July). The maximum and minimum temperatures recorded from 2003 to 2019 were 41.4 °C in July 2010 and -10 °C in January 2008, respectively.

Geology and Hydrogeology

Soft and hard formations in this area exhibit a wide range, from recent alluvium to Camberian crystalline rocks. The alluvium comprises sands of varying sizes, predominantly medium to fine, interspersed with interlayers of salty and gypseous silt and clay. The fine-grain size deposits cover a significant portion of the mining area and appear to prevent direct rainwater infiltration, causing floods in the wet season. The alluvium thickness varies considerably from the northern (30–40 m) to the southern (200–250 m) parts of the mine (Fig. 2). The results of 30 Lefranc tests conducted at 21 boreholes around the mine pit showed that the average transmissivity coefficient (T) in unconsolidated deposits was less than 1 m^2/day. Since the alluvial aquifer is located at the end (outlet) of the hydrological basin, the low hydraulic coefficients have been attributed to the fine grain size of the sediments that are found in this area. The predominant crystalline formations in the study area consist of magnetite, conglomerate, gneiss, schist, and skarn. Gneiss typically contains minerals such as feldspar (albite, orthoclase, and microcline), quartz, muscovite, sericite, and mafic minerals (biotite, pyroxene, and amphibole). Schist is characterized by a mineral assemblage comprising amphibole, calcite, quartz, feldspar (albite and oligoclase), zoisite, clinozoisite, epidote, chlorite, sericite, muscovite, and apatite. Fig. 2 illustrates two geological cross-sections extending east-west (E-W) and north-south (N-S) of the Goharzamin mine area.

As shown in Fig. 1, the region is marked by active faults, and the mining area is confined by the Bibimako thrust fault in the north and the Baghat thrust fault in the south. These faults and their fracture zones are largely responsible for controlling the occurrence of groundwater in the consolidated formations. The permeability characteristics of crystalline formations were measured directly via 376 Lugeon tests in 166 boreholes, with the findings summarized in Table 1. The results mostly exhibit low permeability for different layers, except in instances where fractures are present.

Kheirabad Playa (Fig. 1) is situated approximately 13 km away on the northern boundary of the Goharzamin mine. The playa is covered by evaporite layers, and it experiences a significant amount of runoff during the rainy seasons, leading to the creation of a salt lake on its surface. Because of the region's exceptionally high rate of evaporation, the playa dries up during the warmer seasons. Notably, the Kheirabad strike-slip fault extends from the western boundary of the playa to the eastern vicinity of the Goharzamin mine.

Based on the previous researches (Heidarinejad et al. 2017; Assari 2019; Gharaat et al. 2022), at least two main aquifers (alluvial and fractured aquifers) have existed in the area. However, due to the artesian occurrences in and around the mine pit, this number is not accurate. Based on the field observations of the mine pit walls, alluvial and hardrock aquifers are hydrologically separated by a relatively thick marl layer (15 m) at the bottom of the alluvial (Assari 2019). The spatial extent of this marl layer remains uncertain, implying that hydraulic connectivity between the alluvial and hardrock aquifers is likely limited to areas where the marl unit is either missing or disrupted due to tectonic activities. Moreover, the presence of fine-grained interlayers complicates the precise quantification of aquifers in the alluvial sediments.

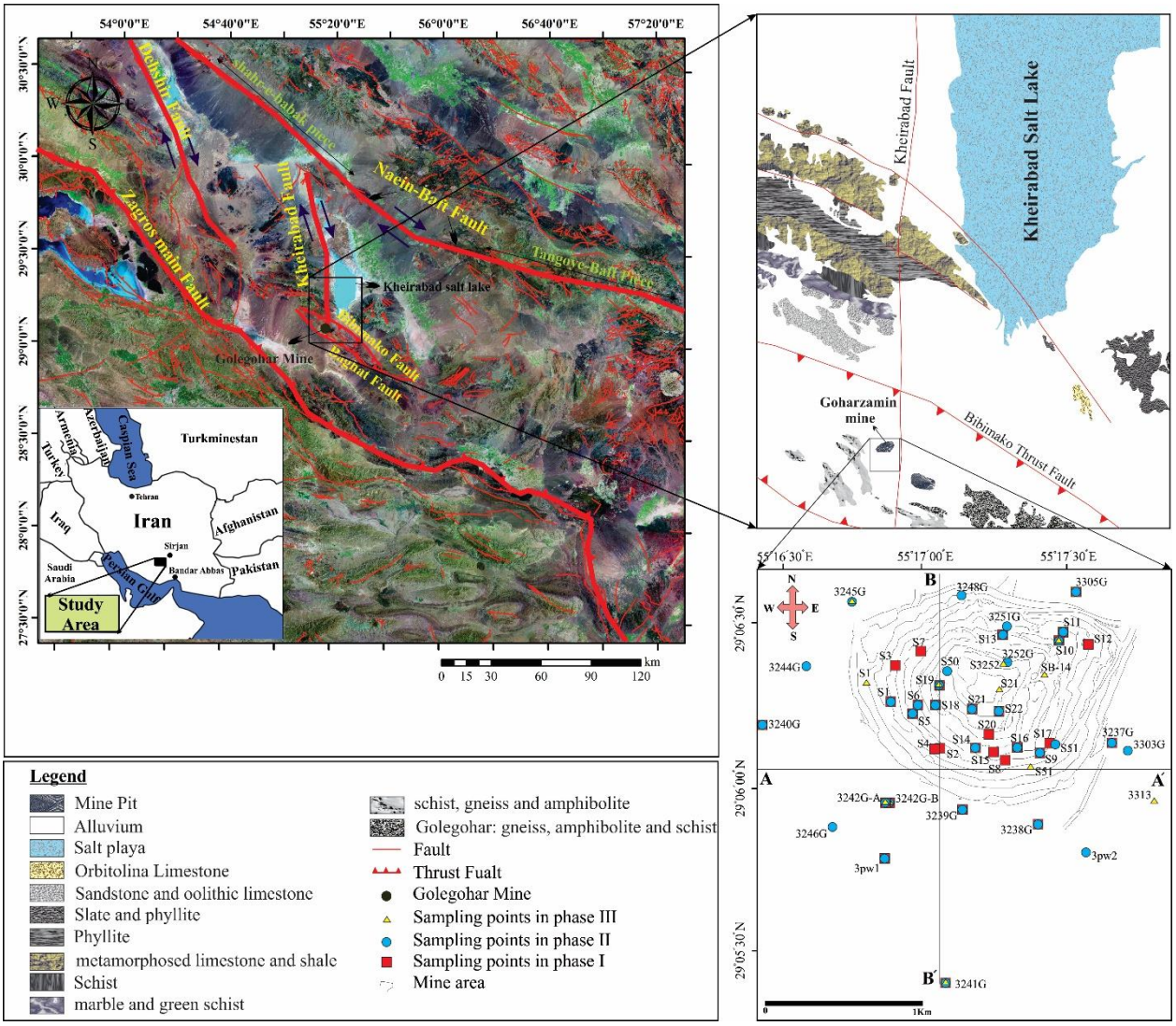

Fig. 1 Geological layers and structures of the research area with sampling locations

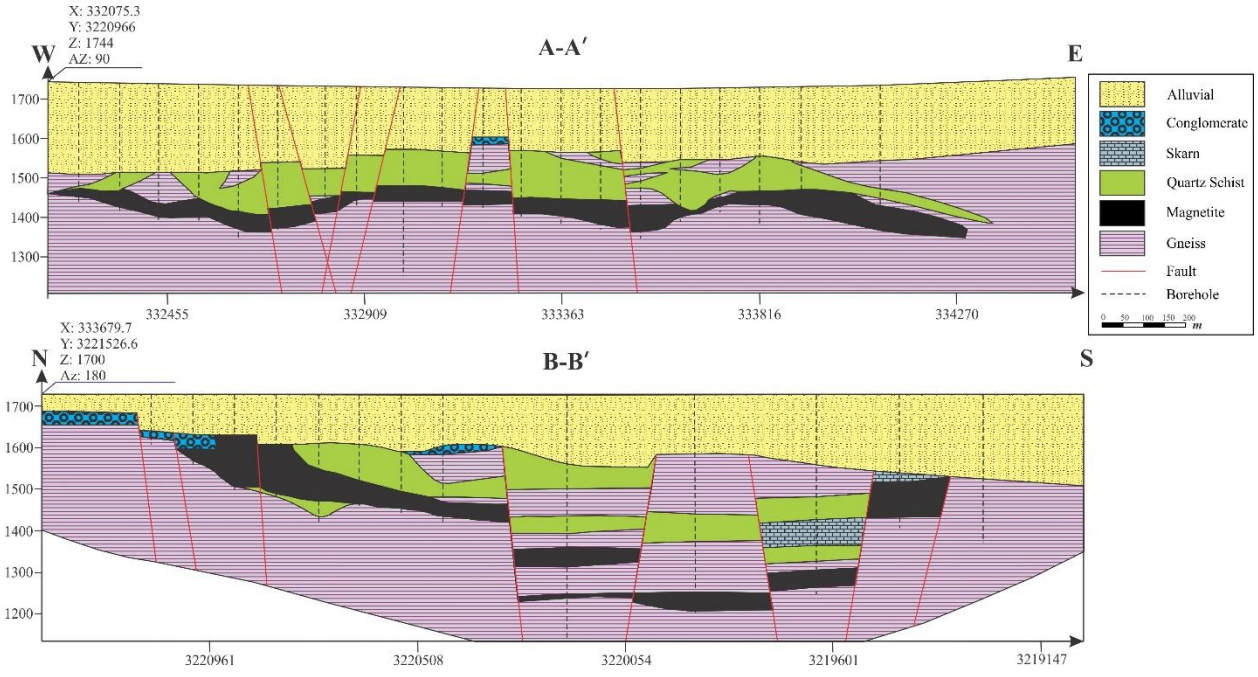

Fig. 2 Geological sections of Goharzamin mine area

Table 1 The permeability and Lugeon values of different rock layers in the Goharzamin mine

Lithology	permeability (m/day)			Lug.			Test
	Min	Ave.	Max	Min	Ave.	Max	frequency
Geniss	0.00	0.02	0.17	0.05	2.01	14.89	126
Schist	0.00	0.03	0.19	0.02	2.75	16.25	53
Magnetite	0.00	0.04	0.22	0.00	3.38	18.33	31
Conglomerate	0.00	0.04	0.12	0.24	3.82	10.17	22
Contact of layers	0.00	0.03	0.29	0.01	2.61	24.07	144

Materials and Methods

Sampling

Groundwater sampling from seepages and boreholes was conducted in three distinct phases, resulting in a total of 75 samples being collected to analyze the spatio-temporal variations of hydrochemical constituents in and around the mine pit. These samples were collected in October 2016, which is referred to as the dry season (phase I: 30 samples), February 2017, which is referred to as the wet season (phase II: 33 samples), and November 2017, which is almost the end of the dry season (phase III: 12 samples) (Fig. 1). To measure the cations and anions, about 250 ml of groundwater were filtered (<0.45 μm) and then collected from sampling network points in polyethylene bottles, separately. In each sampling step, they were thoroughly and carefully washed several times with deionized water. At the sampling points, to prevent any precipitation, the pH of the groundwater samples that were collected for cation measurement was brought below 2 using nitric acid. The anionic samples, however, were not made acidic. The EC and pH were determined by a portable multimeter. Great effort was made to ensure that sampling, preservation, and transport conformed to the guidelines outlined by APHA-AWWA-WPCF (2005). ICP-AES with a LOD (limit of detection) of 0.005 mg/L was employed to measure the main cations (such as calcium and sodium). The trace metal contents were determined by ICP-MS, and anions were determined by SUB-999. The accuracy of the cation and anion results was evaluated by assessing the charge balance error percentage. The samples were in the range of ±5% accuracy, except for samples of S7, S8, S10, S11, S12, S16, and S22 in the dry season, which exhibited an error lower than 10%.

During phase III, a total of 12 groundwater samples for stable isotope ratios ($^{2}H/^{1}H$, $^{18}O/^{16}O$) were collected in 60 mL PET bottles in duplicate. Additionally, 5 samples were collected for each ^{14}C, $\delta^{13}C$, and tritium (^{3}H) analysis in 1-L, 12-mL, and 600-mL PET bottles, respectively. The isotope samples were unfiltered and stored in the dark with zero head space and no preservatives. The testing of the isotopes was implemented at the University of Waterloo in Ontario, Canada. The isotopic compositions of 18O and 2H are presented in relation to the Vienna Standard Mean Ocean Water (V-SMOW), with respective uncertainties of ±0.8 and ±0.2 for 2H and 18O, respectively. The concentration of ^{14}C and ^{3}H is denoted as percent modern carbon (pmc) with analytical uncertainties of 1σ and tritium units (TU) with a precision of ± 0.8 TU, respectively.

Multivariate statistical analysis

Determining the various processes affecting groundwater quality is extremely difficult. Due to numerous chemical variables, different sampling points, and diverse hydrochemical processes, hydrogeochemical studies are by nature a multivariate problem (Chai et al. 2020; Sidhu et al. 2024). Numerous studies have employed multivariate statistical techniques, including PCA and HCA (Samtio et al. 2023; Aduojo et al. 2024), to evaluate water-rock interaction, identifying the source of groundwater and the processes affecting groundwater quality. This research used PCA-HCA techniques to classify the data into groups of related variables and to determine the environmental processes occurring in the aquifers.

In the present research, the PCA statistical method was chosen to explain the chemical processes of groundwater in the mine aquifers. The reliability of the results was evaluated with the Kaiser-Meyer-Olkin (KMO) coefficient. In samples from phases 1 and 2, KMO exhibits a coefficient of about 0.71, indicating that the used statistical method is valid. However, the coefficient in samples from phase 3 was less than 0.5, and PCA was invalid (Abdrabo et al. 2023). To determine the optimal number of PCs, two common methods, including the "scree plot" (Cattell 1966) and the "Kaiser criterion" (Kaiser 1960), were used.

The HCA method was employed to divide the large data into smaller groups based on their hydrogeochemical similarities (Helstrup et al. 2007; Bhatt et al. 2021; Mohammed et al. 2023). To achieve this objective, HCA was implemented by combining Ward's technique and squared Euclidean distance, a widely employed approach for determining dissimilarity (Rahman et al. 2021; Feisal et al. 2023). The standardization of chemical parameter concentrations between 0 and 1 was achieved using the Z-score method.

The statistical methods (in SPSS software) were initially employed to analyze the groundwater geochemistry data. Subsequently, the processes influencing the groundwater quality in the region were investigated via the utilization of geochemical plots (AquaChem 12 and Excel 2013 software). In phases 1 and 2, about 15 qualitative parameters (Na, K, HCO3, Cl, Ca, Mg, SO4, F, NO3, N (nitrite), TH, Alk, pH, TDS, and EC) were employed for both statistical methods, showing moderate to high correlation with each other. However, in phase 3, HCA was applied using the 35 selected characteristics (EC, Alk, K, Na, Mg, Ca, SO4, HCO3, Cl, NO3, N, Ba, F, B, Cr, Co, Cs, Eu, Li, Cu, Mn, Ni, Pd, Mo, Rb, Re, Sb, Si, Sn, U, Y, Zn, Br, Sr, and As).

Results and discussion

Main ion composition

Geochemical analyses of groundwater samples from the Goharzamin mine were conducted in three phases (dry and wet seasons, as well as a supplementary sampling phase) and subjected to initial statistical assessment, as presented in Tables 2 and 3. The extensive range of hydrochemical data observed in the tables may be attributed to different groundwater sources. The mean values of EC are equal to 48.39 to 58.57 mS cm^{-1} in dry and wet seasons, respectively, indicating a significant concentration of soluble characteristics in the mine groundwater. In the dry season (phase 1), the maximum of EC belongs to the samples S19, S22, S21, and 3242G-B with values of 167.8, 140.3, 137, and 123.6 mS cm^{-1}, respectively. The concentrations of main cations, including Ca^{2+}, Mg^{2+}, K^{+}, and Na^{+}, lie between 200 to 16032, 24 to 4800, 50 to 940, and 595 to 27420 mg L^{-1}, respectively, with mean values of 4069.03, 765.03, 140.33, and 6113 mg L^{-1}, in that order. The abundance of cations from high to low is as follows: Na^{+}-Ca^{2+}-Mg^{2+}-K^{+}. The highest Na content belongs to S22, S21, 3242G-B, and S10 samples, with values of 27420, 22540, 21329, and 18876 mg L^{-1}, respectively.

The HCO_3^-, Cl^-, SO_4^{2-}, and NO_3^- main anions varied from 7 to 122, 1106 to 69680, 124 to 1025, and 3 to 135 mg L^{-1}, respectively, with an average of 46.99, 19487.97, 686.97, and 40.46 mg L^{-1}, in that order. The ranking of anion abundance is observed as $Cl^- > SO_4^{2-} > HCO_3^- > NO_3^-$. Samples S22, S21, 3242G-B, and S10 have the highest Cl concentrations, measuring 69680, 68837, 57694, and 53274 mg L^{-1}, respectively.

Analysis of samples during the wet season (phase 2) indicates that EC demonstrates the widest range (164470 µS cm^{-1}). Among the samples, the highest EC belongs to S19, 3252G, S50, S22, and S21, with values of 169, 142.8, 138.8, 135.5, and 130.6 mS cm^{-1}, respectively. The dominant anion and cation during this phase are Cl and Na, with mean concentrations of 20863.38 and 10563.81 mg L^{-1}, respectively. The order of cation and anion abundance remains consistent with that of phase 1. Wet season samples exhibited higher concentrations of Na, Cl, K, TDS, EC, and HCO3, which may be attributed to the dissociation and dissolution processes of evaporates in the aquifer.

According to the geological sections (Fig. 2), the high Cl concentrations observed in mine groundwater samples may be attributed not only to the dissolution of evaporites in alluvium but also to the weathering processes affecting metamorphic rocks such as Schists and Gnisses. Krimissa et al. (2004) proposed that the weathering of biotite and other unidentified Cl minerals in the schist rocks at the plain of Chtouka-Massa was responsible for the high Cl concentration (about 4300 mg/L) in groundwater. This hypothesis was claimed based on empirical measurements showing high Cl values in leachates derived from schist rock.

Fluoride concentrations in groundwater samples differ from 0.06 to 1.61 mg/l (with an average of 1.06 mg/L) and 0.27 to 1.56 mg/l (with an average of 0.93 mg/l) in phases 1 and 2, respectively. The concentration of fluoride ions exceeds the recommended limit (about 1.2 mg L^{-1}) in the WHO standard (2006) for potable water in 47% and 31% of the dry and wet season samples, respectively. The high fluoride concentrations are likely attributed to mineral weathering processes including mica (muscovite and biotite), apatite, fluorite, and other fluoride-bearing minerals that are abundant in gneiss and other metamorphic rocks found in the area.

The nitrate values in Goharzamin mine water samples were found to be moderately high. In phase 1, the NO_3^- concentration ranged from 3 to 135 mg/l, with an average of 40.46 mg/l, while in phase 2, the concentration varied from 9 to 69 mg/l, with a mean value of 31.44 mg/l. The main sources of NO_3^- in groundwater, as indicated by Moloantoa et al. (2022); and Boumaiza et al. (2023), include industrial wastewater, rainfall, biological nitrogen fixation (BNF), and the application of nitrogenous fertilizers.

Table 2 Statistical analysis of Goharzamin mine groundwater

	Dry Season (phase 1)					Wet Season (phase 2)				
	Mean	**Range**	**Min**	**Max**	**count**	**Mean**	**Range**	**Min**	**Max**	**count**
Ca (mg/l)	4069.0	15832.0	200.0	16032.0	30	2281.4	9018.0	200.0	9218.0	32
Mg (mg/l)	765.0	4776.0	24.0	4800.0	30	323.7	1176.0	24.0	1200.0	32
Na (mg/l)	6113.0	26825.0	595.0	27420.0	30	10563.8	44289.0	385.0	44674.0	32
K (mg/l)	140.3	890.0	50.0	940.0	30	297.3	1374.0	15.0	1389.0	32
HCO3 (mg/l)	47.0	115.0	7.0	122.0	30	64.5	114.0	10.0	124.0	32
SO4 (mg/l)	687.0	901.0	124.0	1025.0	30	585.9	1101.5	12.5	1114.0	32
Cl (mg/l)	19488.0	68574.0	1106.0	69680.0	30	20863.4	75394.0	754.0	76148.0	32
TDS (mg/l)	32794.0	106334.0	2736.0	109070.0	30	44340.5	139284.0	3114.0	142398.0	32
EC (mS/cm)	48.4	163.1	4.7	167.8	30	58.6	164.5	4.5	169.0	32
pH	7.6	1.5	6.7	8.2	30	7.4	3.0	6.0	9.0	32
F (mg/l)	1.1	1.6	0.1	1.6	30	0.9	1.3	0.3	1.6	32
N (mg/l)	19.9	92.0	3.0	95.0	30	14.2	26.0	6.0	32.0	32
TH (mg/l)	13890.3	59060.0	940.0	60000.0	30	7092.5	27000.0	1000.0	28000.0	32
Alk (mg/l)	38.7	79.6	5.4	85.0	30	53.1	94.0	8.0	102.0	32
NO3 (mg/l)	40.5	132.0	3.0	135.0	30	31.4	60.0	9.0	69.0	32
Elevation (mamsl)	1663.4	184.0	1563.0	1747.0	30	1579.5	472.1	1259.9	1732.0	32

Table 3 Statistical analysis of Goharzamin mine groundwater in Supplementary phase (phase III)

	Mean	**Median**	**Standard Deviation**	**Kurtosis**	**Skewness**	**Range**	**Min**	**Max**	**count**
Elevation (mamsl)	1518.4	1544.5	125.4	0.0	-0.9	390.0	1260.0	1650.0	12
EC (mS/cm)	79.5	83.1	53.0	-0.1	0.4	181.7	4.0	185.6	12
Alkalinity (total) (mg/l)	39.3	38.6	28.2	1.0	0.9	99.6	3.4	103.0	12
Ca (ppm)	7048.6	6953.9	4674.3	-0.5	0.3	15624.0	247.0	15871.0	12
Mg (ppm)	473.4	520.5	252.7	0.6	0.6	882.5	133.2	1015.7	12
Na (ppm)	14097.1	14650.0	10239.8	0.7	0.7	35778.7	766.3	36545.0	12
K (ppm)	138.2	115.4	109.2	2.0	1.2	396.3	5.0	401.3	12
HCO3 (mg/l)	47.8	47.1	34.2	0.9	0.9	120.9	4.1	125.0	12
SO4 (mg/l)	474.1	392.0	255.0	1.3	1.5	756.0	254.0	1010.0	12
Cl (mg/l)	38516.7	39000.0	27131.2	0.4	0.6	94700.0	1300.0	96000.0	12
NO3 (mg/l)	6.3	4.9	7.0	-1.0	0.6	18.4	0.0	18.4	12
F (mg/l)	0.6	0.6	0.2	-0.6	-0.4	0.5	0.3	0.8	12
N (Nitrite) (mg/l)	0.4	0.0	0.8	5.6	2.4	2.6	0.0	2.6	12
B(ppb)	8601.2	8702.0	5966.2	0.2	0.6	20018.0	1256.0	21274.0	12
Ba(ppb)	1528.2	990.9	1263.3	-0.6	0.7	3911.3	16.8	3928.1	12
Li(ppb)	9891.5	10881.5	7067.0	-1.3	0.0	21464.0	93.0	21557.0	12
Mn(ppb)	3087.2	2774.1	2857.9	0.0	0.9	8837.2	0.8	8838.0	12
Pd(ppb)	100.0	96.4	66.7	-0.9	0.1	216.8	3.1	219.9	12
Rb(ppb)	533.2	435.5	495.1	2.0	1.3	1726.3	6.3	1732.6	12

Si(ppb)	5257.5	5145.0	2231.0	-0.1	0.4	7733.0	1818.0	9551.0	12
Zn(ppb)	94.4	11.5	148.6	1.6	1.7	427.3	<5	431.0	12
Br(mg/l)	24.7	26.1	15.3	-1.6	-0.3	40.6	1.0	41.6	12
Sr(ppm)	337.4	375.5	214.9	-1.1	-0.2	673.5	8.6	682.0	12
Cs(ppb)	135.7	120.8	147.1	1.6	1.2	485.9	0.2	486.1	12
Cu(ppb)	14.8	5.1	17.8	0.6	1.4	49.6	0.9	50.5	12
Mo(ppb)	14.2	9.7	16.6	7.7	2.6	61.6	1.2	62.8	12
Ni(ppb)	12.6	7.1	14.5	2.4	1.5	47.5	1.0	48.5	12
Co(ppb)	4.5	1.5	7.3	4.0	2.2	23.2	0.3	23.5	12
Cr(ppb)	2.0	2.0	1.1	-0.6	0.1	3.5	<0.5	3.9	12
As(ppb)	1.6	1.3	1.0	-0.3	0.8	3.1	<0.5	3.5	12
Sn(ppb)	1.1	0.9	0.9	-0.3	0.8	2.6	0.1	2.7	12
Sb(ppb)	0.9	0.9	0.5	1.0	0.9	1.6	<0.5	2.0	12
U(ppb)	1.1	0.9	1.0	-0.6	0.7	2.8	<0.1	2.9	12
Eu(ppb)	0.2	0.2	0.1	2.2	-0.5	0.2	<0.1	0.3	12
Re(ppb)	0.3	0.1	0.5	10.7	3.2	1.7	<0.04	1.7	12
Y(ppb)	0.4	0.2	0.6	6.8	2.6	1.9	<0.1	2.0	12

A piper diagram (Fig. 3) was drawn to determine the water type and hydrochemical facies (Dhurandhar and Ranjan 2020). The groundwater types and facies provide insights into the flow patterns of contained water and the influence of hydrochemical processes occurring in the lithological environment (Back 1966; Ophori and Toth 1989). According to the relative predominance of main ions with regards to their reacting values, three distinct groundwater types have been distinguished in the Goharzamin mine area, ranging from relatively saline (or brackish) groundwater (mixed-Cl) to high saline groundwater (Na-Cl) (Fig. 3 and Table 4), as follows: 1) sodium chloride (Na-Cl, 49 samples), which is highly mineralized in the mine area, especially at greater depths, suggesting that the groundwater has a considerable residence time and movement or relatively strong rock-water interactions. 2) Neutral cation-chloride (Mixed-Cl, 12 samples), characterized by lower mineral content compared to the previous type, typically found in shallow depths of the alluvial aquifers; and 3) Calcium chloride (Ca-Cl, 13 samples), which probably results from the mixing of waters from conglomerate (containing calcite cement) or calcite-dolomite formations with saline waters. Moreover, higher Ca concentrations may be attributed to the reverse exchange of the ions between clay interlayers and saline water. If the saline water infiltrates the alluvial aquifer, Na is adsorbed on the clay surface, releasing Ca and leading to the occurrence of Ca-Cl water type.

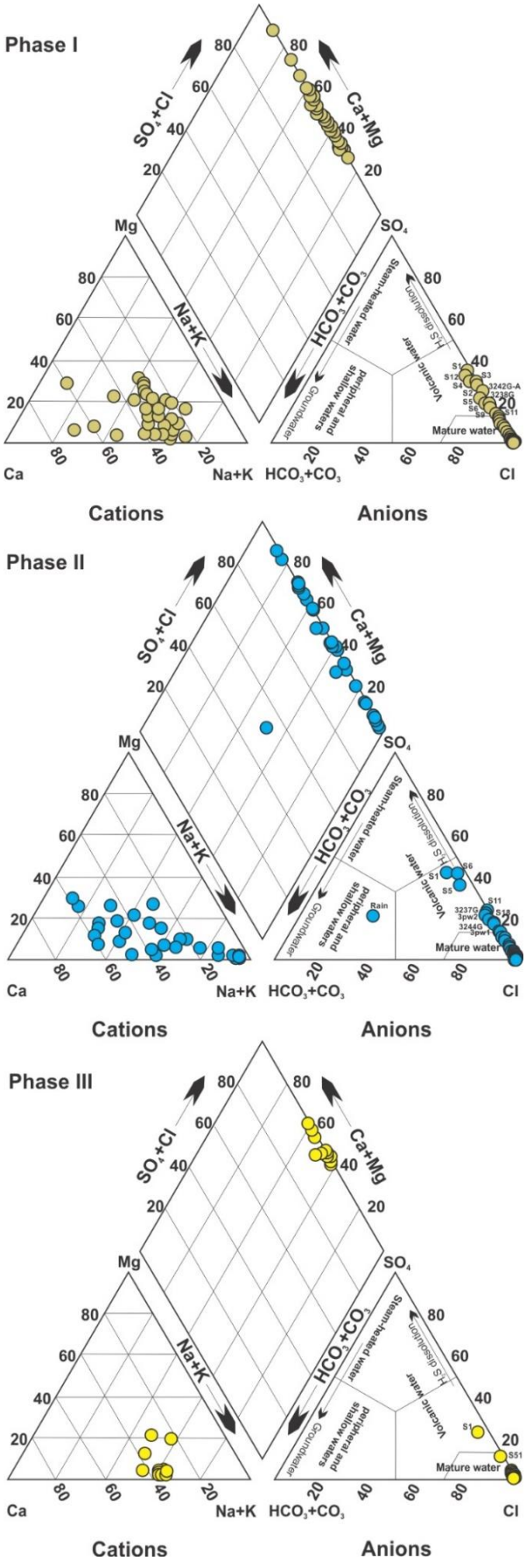

Fig. 3 Piper plot. (a) phase I; (b) phase II; and (c) phase III

Table 4 Types of hydrochemical facies in Goharzamin mine groundwater samples

Phase I		Phase II		Phase III	
Sample ID	**Water type**	**Sample ID**	**Water type**	**Sample ID**	**Water type**
S1	Na-Ca-Cl-SO4	S1	Na-Ca-Cl-SO4	S1	Na-Ca-Cl-SO4
S10	Na-Ca-Cl	S10	Na-Cl	S10	Na-Ca-Cl
S19	Ca-Mg-Cl	S19	Na-Cl	S19	Na-Ca-Cl
S21	Na-Ca-Cl	S21	Na-Cl	S21	Na-Ca-Cl
3242G-A	Mixed-Cl	3242G-A	Mixed-Cl	3242G-A	Na-Ca-Cl
3242G-B	Na-Ca-Cl	3242G-B	Na-Ca-Cl	3242G-B	Na-Ca-Cl
3241	Na-Ca-Cl	3241	Ca-Na-Cl	3241	Na-Ca-Cl
S5	Na-Ca-Cl-SO4	S5	Mixed-Cl-SO4		
S6	Na-Ca-Cl	S6	Na-Ca-Cl-SO4		
S9	Mixed-Cl	S9	Na-Cl		
S11	Na-Ca-Cl	S11	Na-Ca-Cl		
S13	Ca-Na-Cl	S13	Na-Cl		
S14	Na-Ca-Cl	S14	Na-Ca-Cl		
S16	Na-Ca-Cl	S16	Na-Cl		
S18	Na-Ca-Cl	S18	Na-Ca-Cl		
S22	Na-Ca-Cl	S22	Na-Cl		
3pw1	Ca-Na-Cl	3pw1	Ca-Mg-Cl		
3237G	Na-Ca-Cl	3237G	Mixed-Cl		
3238G	Na-Ca-Cl	3238G	Na-Cl		
3239G	Na-Ca-Cl	3239G	Ca-Na-Cl		
3240	Ca-Na-Cl	3240	Ca-Na-Cl		
S2	Na-Ca-Cl-SO4	S51	Na-Ca-Cl	S51	Mixed-Cl
S3	Na-Ca-Cl-SO4	3245	Na-Cl	3245	Na-Ca-Cl
S4	Na-Ca-Cl-SO4	3252	Na-Cl	3252	Na-Ca-Cl
S7	Mixed-Cl	3244	Ca-Mg-Cl	3313	Na-Ca-Cl
S8	Mixed-Cl	3pw2	Mixed-Cl	SB-14	Na-Ca-Cl
S15	Na-Ca-Cl	3246	Ca-Na-Cl		
S12	Mixed-Cl-SO4	3248	Mixed-Cl		
S17	Mixed-Cl	3305	Ca-Na-Cl		
S20	Na-Ca-Cl	3251	Ca-Na-Cl		
		3303	Ca-Na-Cl		
		S50	Na-Cl		

Hierarchical cluster analysis

To better understand the relationships and patterns within the normalized data, hierarchical cluster analysis (HCA) was executed. Fig. 4 exhibits the HCA statistical method dendrogram for the classification of the samples. Based on their hydrochemical signature and dominant chemical composition, samples with a rescaled distance of less than 12 were classified together to form chemically distinct clusters. As reflected in Fig. 4, the samples are placed in two distinct clusters (C1 and C2) in each phase, although they may be further subdivided into three or four clusters at lower rescaled distances. In phase 1, the samples of 3237G, 3240, 3242G-B, S19, S21, and S22 were placed in C2, while C1 is composed of S1 to S18, S20, 3239G, 3242G-A, 3238G, 3pw1, and 3241. In phase II, the samples of S1, S5, S6, S9, S11, S14, S16, S18, S51, rain, 3244, 3pw1, 3237G, 3pw2, 3242G-A, 3245, 3248, 3305, 3239G, 3241, and 3251 were classified in C1, whereas C2 includes the samples of 3240, 3303, S13, 3238G, S19, S50, S10, 3245, S21, S22, 3252, and 3242G-B. It should be mentioned that in the samples of each cluster, similar chemical processes affect water quality. According to the rescaled distance, As shown in Figure 4, it is clear that the similarity among the samples increases during phase 2 (the wet season). Moreover, by comparing the same samples from phase 1 to phase 2, it can be seen that the sample of 3237G shifts from C2 to C1, and S10, S13, and 3238G shift from C1 to C2. These shifts are attributed to changes in hydro-geochemical mechanisms, including water mixing, ion exchange, mineral dissolution, and so on, at the sampling sites. In three phases, two samples of 3242G-A and 3242G-B lie in completely different clusters. The considerable proximity of these samples, along with variations in their depth, suggests the action of different mechanisms influencing water chemistry with respect to depth.

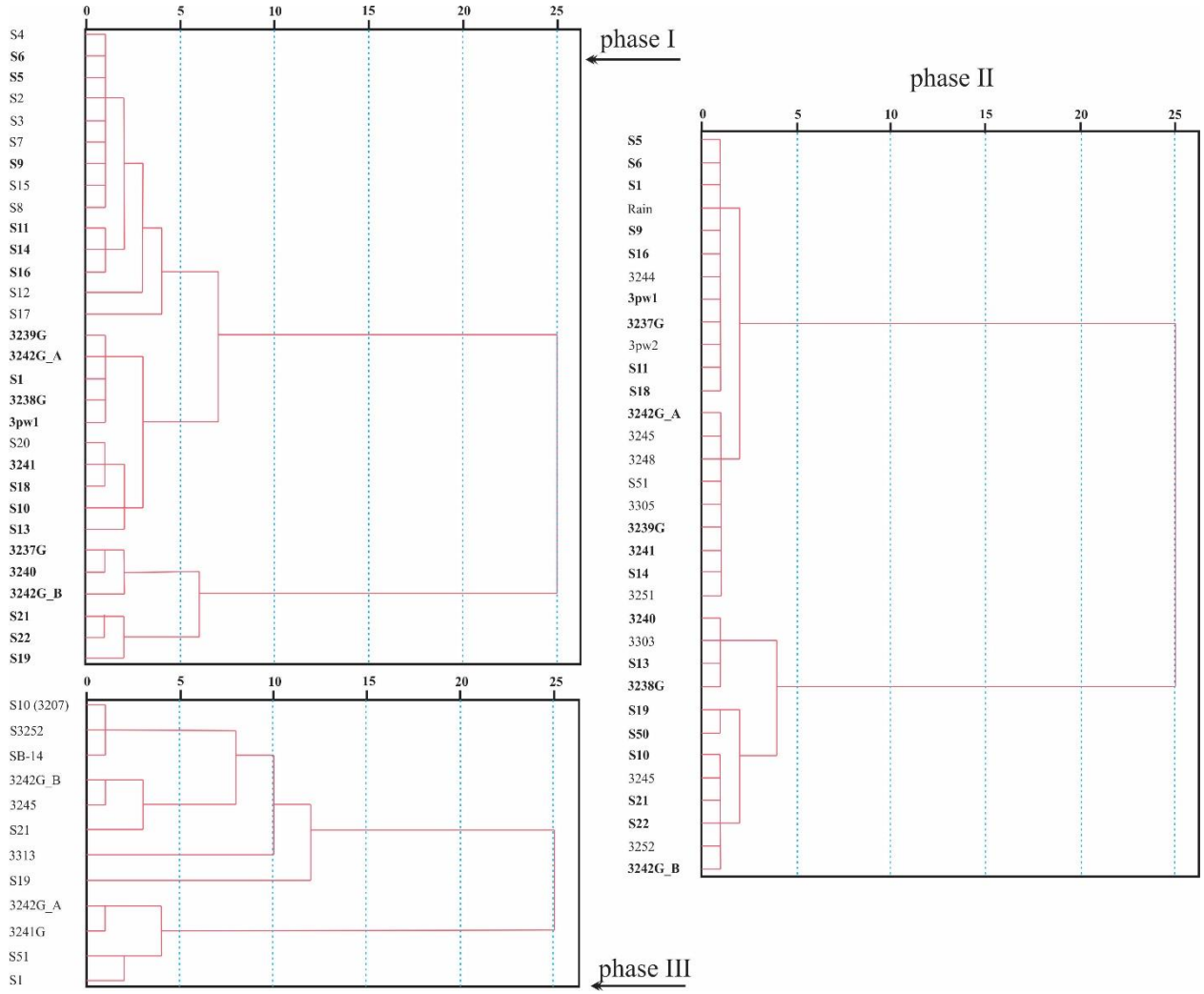

Fig. 4 Dendrogram of HCA statistical method (Ward's technique) for the groundwater samples considered in mine groundwater samples

Principal component analysis (PCA)

Individual and cumulative explained variances, loading of qualitative variables, and eigenvalues obtained by principal component analysis for the samples collected during phases 1 (dry season) and 2 (rainy season) are displayed in Tables 5 and 6. Total variable loadings are also presented in Tables 5 and 6. For the final analysis, loadings greater than 0.5 and less than -0.5 were used.

In phase 1, three principal rotated components (RCs) account for about 77% of the cumulative explained variances (Table 5). The RC1 and RC2 individual principal components describe approximately 45% and 23% of the cumulative explained variances, respectively. The water quality in the mine aquifers is primarily governed by these two RCs. Since RC3 only contributes approximately 9% of the overall data variance, compared to the previous two RCs, it is less significant and is more likely to be attributable to local impacts.

Variables such as EC, K, Na, Mg, Ca, TDS, Cl, SO4, and TH in RC1 are positively correlated. In addition, pH is negatively correlated with RC1. Na^{+}-Cl^{-} and Ca^{2+}-SO_4^{2-} are ion pairs highly correlated in RC1, originating from the same sources. These physicochemical variables, which account for about 45% of the cumulative explained variance, are abundant ions in the halite and gypsum interlayers of alluvial deposits in the Goharzamin mine area. EC and TDS have a positive and significant correlation with RC1, suggesting that this rotated component may be known as a salinization dimension or salinization process in the mine area. Also, the high positive loading of Mg and Ca in RC1 can be caused by the effect of reverse ion exchange processes of alkali earth metals by alkali metals.

HCO_3, Alk, and NO_3 are found to have moderate-to-high negative loadings in RC2. F also exhibits moderate and positive loading (0.51) in RC2. RC3 is characterized by a moderate-to-high loading of NO_3 and N. As previously mentioned, the main source of F is Gniess and other metamorphic rocks in the area. The main source of NO_3 is also anthropogenic activity. Thus, RC2 and RC3 relate to geogenic and anthropogenic mechanisms.

Three RCs were also extracted in phase 2, accounting for 79% of the total data variance (Table 6). RC1 exhibits a strong correlation with Na, Cl, and K, influencing over 35% of the total explained variance. Moreover, RC1 had a significant and positive correlation with TDS and EC, suggesting a considerable influence on the water quality of samples collected from the mining area. RC2 is associated with the TH, Ca, Mg, and N variables, showing positive loadings between 0.68 and 0.94. They explain around 24% of the total data variance. RC3 is linked to the hydrochemical components of Alk, NO_3, SO_4, HCO_3, and F with a moderate to high loading ranging from 0.51 to 0.81, accounting for 20% of the full variance.

In phase 2, two rotated components (RC1 and RC2) explain around 59% of the full data variance. By comparing the variables in the first two RCs (RC1 and RC2) in Phase 2 and RC1 in Phase 1, it can be concluded that halite dissolution or probably the intrusion of saline water (possibly from Kheirabad playa) are the main factors influencing the chemical composition of Goharzamin mine groundwater samples in rainy seasons.

Table 5 Individual and cumulative explained variances, and loading of qualitative parameters in the dry season

Physicochemical parameters	Component		
	RC1	RC2	RC3
pH	**-.75**	-.11	-.09
EC	**.87**	.38	.10
TDS	**.84**	.41	.18
TH	**.85**	.18	.01
Alk	-.15	**-.94**	-.10
Ca	**.82**	.43	.14
Mg	**.90**	.09	-.09
NO3	-.42	**-.53**	**.59**
SO4	**-.63**	-.48	.12
Cl	**.86**	.40	.19
HCO3	-.12	**-.95**	-.05
F	**.51**	**.57**	-.01
N	.23	.19	**.91**
Na	**.71**	.39	.24
K	**.54**	-.03	-.10
Eigenvalues	6.70	3.52	1.39
% Variance explained	44.64	23.44	9.24
% Cumulative variance	44.64	68.09	77.33

Extraction Method: Principal Component Analysis.
Rotation Method: Varimax with Kaiser Normalization.[a]
a. Rotation converged in 4 iterations.

Table 6 Individual and cumulative explained variances, and loading of qualitative parameters in the wet season

Physicochemical parameters	Component		
	RC1	RC2	RC3
pH	-.48	-.04	.48
EC	**.93**	.23	-.23
TDS	**.93**	.19	-.25
TH	.02	**.94**	.11
Alk	-.46	.01	**.81**
Ca	.09	**.94**	.06
Mg	-.15	**.92**	.05
NO3	-.12	.36	**.73**
SO4	**-.50**	.13	**.60**

Cl	**.94**	.16	-.22
HCO3	-.46	.01	**.81**
F	.43	-.38	**.51**
N	.26	**.68**	.004
Na	**.94**	-.04	-.24
K	**.78**	-.23	-.26
Eigenvalues	5.31	3.54	3.00
% Variance explained	35.42	23.63	19.97
% Cumulative variance	35.42	59.05	79.02

Extraction Method: Principal Component Analysis.
Rotation Method: Varimax with Kaiser Normalization.[a]
a. Rotation converged in 6 iterations.

Hydrochemical evolution and the origin of groundwater

Precipitation, parent rock composition, weathering, the interaction between aquifer materials and water, dissolution, evaporation, and time affect the chemical evolution of groundwater. (Saberinasr et al. 2019; Subba Rao et al. 2020).

Two diagrams were introduced by Gibbs (1970) to identify the relationships between the hydrochemical composition of groundwater and the governing processes (Fig. 5). According to the source of ions and the processes controlling water chemistry, Gibbs diagrams are divided into three parts, including rock-groundwater interaction, precipitation, and evaporation (Liu et al. 2023; Mussa and Mjemah 2023). The water samples collected from Goharzamin mine were positioned predominantly at the top right of the diagram. These samples exhibited $Cl^-/(Cl^-+HCO_3^-)$ and (Na+K)/(Na+K+Ca) ratios exceeding 0.5, as well as a TDS value exceeding 1000 mg/L. These findings indicate that the composition of main ions in the mine's groundwater is primarily influenced by evaporation and mineral crystallization processes, rather than interactions between the water and surrounding rocks or precipitation.

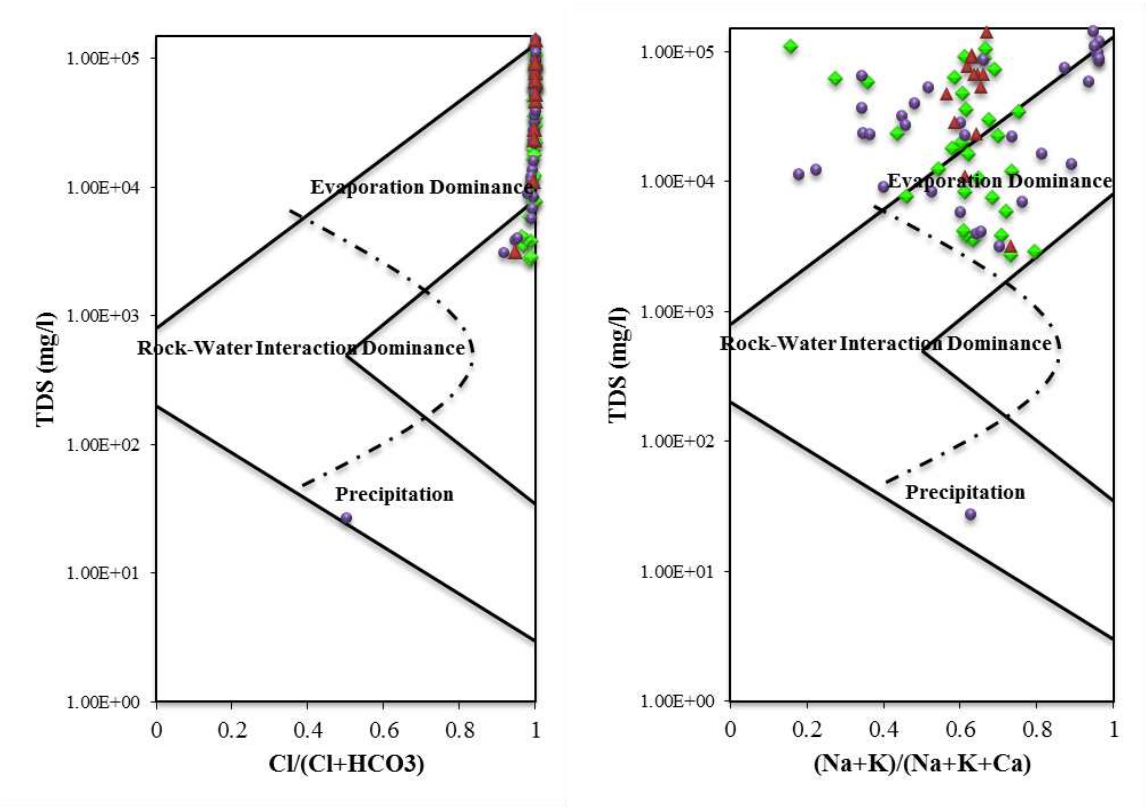

Fig. 5 Gibbs Plot

In determining the qualitative components of groundwater, factors such as topography, lithology, and depth of groundwater have a significant role. Fig. 6 presents a link between EC and the depth of mine

groundwater samples (EC-depth plot). The diagram reveals the existence of three or four distinct clusters among the samples, potentially attributed to the effect of different aquifer types. The shallower samples exhibit a broad range of EC values (~4 to ~105 mS cm^{-1}), which can be classified as samples with very low to low EC and samples with medium to high EC. The samples with lower EC can be linked to recharge by new meteoric water or new precipitation, while the samples with higher EC may be associated with evaporite dissolution, mixing meteoric and saline water, or salt water intrusion. In contrast, deeper samples display medium (approximately 50 mS cm^{-1}) to very high values of EC (~ 100 mS cm^{-1} <), which is probably due to the high groundwater residence time and water-rock interactions.

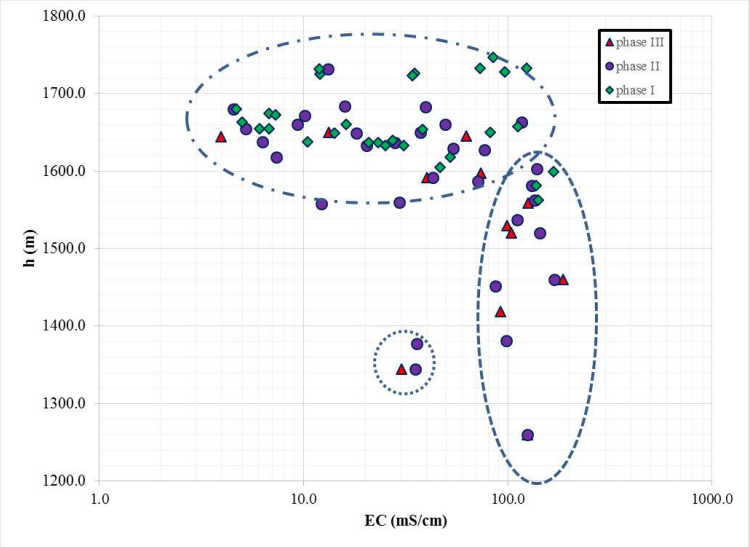

Fig. 6 Variations of EC of Goharzamin mine groundwater samples (mS/cm) with sampling level (m)

The classification of groundwater samples was conducted by assessing their principal cations and anions, as well as calculating the reaction values (relative percentages), as depicted in Figure 7 (Barbieri et al. 2005). The samples were classified into two types: Ca + Mg – SO4 – Cl and Na + K – SO4 – Cl. These water types are consistent with the geological formations of the area. Based on the graph (Fig. 7), most of the cation composition of mine groundwater samples changed into Na + K in the wet season as the water became more saline. For instance, in the sample of S19 (collected from an artesian borehole) during the dry season (phase I), the dominant cation composition and EC were Ca + Mg and 167.8 mS cm^{-1}, respectively. While, during the wet season (phase II), EC had an increase in value (169 mS cm^{-1}), and the dominant cation composition shifted to Na + K. In phase III, a substantial increase in EC was observed (185.6 mS cm^{-1}), which is due to the decrease in the number of surface samples. In this phase, the dominant cation composition was positioned in the middle of the Na + K and Ca + Mg axes. Variations in dominant cation composition were observed in samples S10 and S13 from artesian sources. These findings suggest that the artesian aquifer may not be completely isolated, suggesting a potentially restricted hydraulic connection between the aquifers. However, an investigation of the groundwater in the piezometers exhibited that the groundwater level in the hard crystalline layer is higher than the alluvium layer among just some of the piezometers adjacent to the mine pit. This artesian condition is probably due to the mine floor excavation and a consequence of a very high hydraulic gradient. In this situation, the faults and fractures act as a groundwater flow passage, allowing for rapid discharge under pressure. In addition, the creation of unloading joints or release joints occurs as a consequence of decreased overburden pressure and an increased depth of the mine pit. The mentioned faults and joints near the mine pit have the potential to facilitate the mixing of water from different sources.

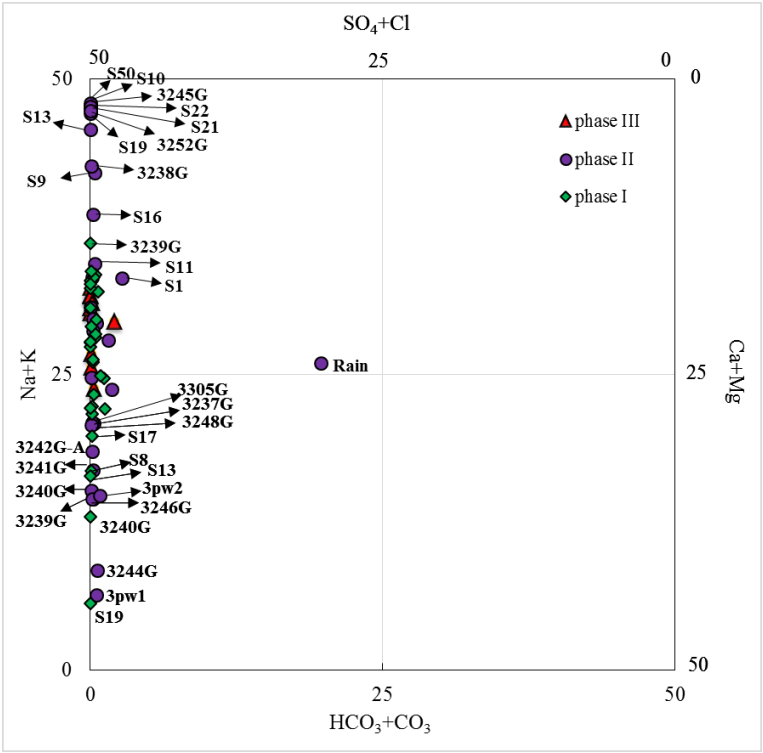

Fig. 7 Reaction values expressed as a percentage of major cation and anion groups. The names of all the gathered groundwater samples are displayed

Cl and Br are considered conservative tracers, which means that once in solution, they are resistant to removal by the majority of processes, with the exception of precipitation during the final stages of salinization. Consequently, they could reflect water quality changes and their origins with less ambiguity than other dissolved species. This characteristic has made the Cl/Br mass ratio a useful tool in groundwater for determining the source of salinity (Sophocleous et al. 1990; Whittemore 1995; Rotiroti et al. 2023; Ayari et al. 2023). Some researchers have found that Cl/Br ratios in water can be affected by Br sorption on soil iron oxides and clays (Fabryka-Martin et al. 1991; Whittemore and Davis 1995). Moreover, different ranges of Cl/Br ratios have been reported for a variety of end members that manage salinity mechanisms in water. The Br/Cl vs. B/Cl ratio plot is used to infer the origin of the groundwater in this study (Fig. 8). As depicted in this plot, the majority of mine groundwater samples (phase III) are situated within a limited range of 0.0004 to 0.0015 for the B/Cl ratio and 0.00018 and 0.0003 for the Br/Cl ratio. The plot indicates that all mine groundwater samples may be affected by either evaporite dissolution and/or agricultural drainage. Krimissa et al. (2004) and Ettayfi et al. (2012) have shown waters with high Cl content and a low ratio of Br/Cl ($<1.5\times10^{-3}$) in schist rocks. Consequently, schist rocks could play a role in the salinization of Goharzamin mine groundwater resources, besides evaporite dissolution.

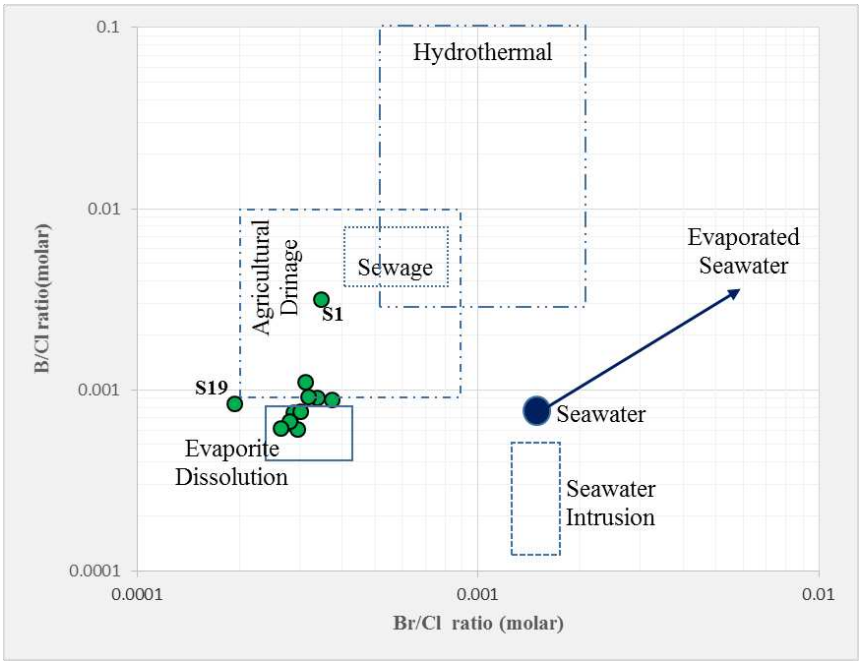

Fig. 8 Ratios of Br/Cl vs. B/Cl

The relationship between Na and Cl, as shown in Figure 9, has often been employed to explain the mechanisms for acquiring salinity in semi-arid climates (Farid et al., 2012). The analysis reveals that the mine groundwater samples exhibit an equal concentration of both ions during the wet season and align with the dissolution line of NaCl (halite) (typical 1:1 stoichiometric line). Consequently, it is inferred that these two elements originate from halite dissolution in the mine area. Conversely, the data from the dry season demonstrates a depletion in Na rather than Cl, suggesting a potential ion exchange between Na and Ca in the environment.

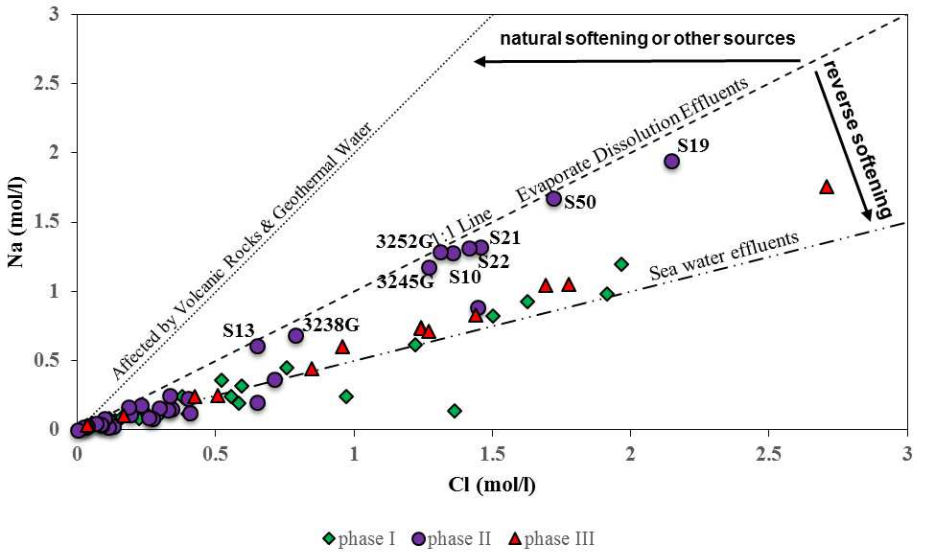

Fig. 9 Na vs. Cl relationship

In the aquifer medium, the primary solute composition of groundwater may experience alterations due to ion exchange, which is a common phenomenon in the geochemical evolution of groundwater. The occurrence of this process in the groundwater is often underlined by the graph of (Ca + Mg) – (HCO3 + SO4) (meq) against (Na + K) – Cl (meq) (Fig. 10), where the water samples are expected to group together along a line with a slope of -1. The scattering of all samples in the upper left quadrant of the plot indicates

an excess of divalent ions and a deficiency of monovalent ones. This means that any variations in the levels of divalent ions are counterbalanced by shifts in monovalent ions.The samples from the area are arranged in a straight line with a 1:-1 ratio (Fig. 10), in accordance with the ideal ion exchange. Consequently, ion exchange emerges as a significant mechanism influencing the composition of the majority of aquifers in the mining area. To deduce the exchange and/or reverse exchange of ions between a fluid and its media during movement or residence times, Schoeller (1967) suggested employing two indexes (CAI_1 and CAI_2), as follows:

$$CAI_1 = \frac{Cl^- - (K^+ + Na^+)}{Cl^-} \quad (1)$$

$$CAI_2 = \frac{Cl^- - (K^+ + Na^+)}{HCO_3^- + SO_4^{2-} + NO_3^- + CO_3^-} \quad (2)$$

The indices are both positive in the reverse ion exchange process between the ions K^+ and Na^+ in the fluid (groundwater) and Ca^{2+} and Mg^{2+} in the media (materials of the aquifer), and vice versa. According to Fig. 10, it can be concluded that the reaction of reverse ion exchange is dominant at three sampling phases (except S1 in phase II). This phenomenon might be attributed to the high concentration of sodium in the groundwater, leading to the displacement of calcium in the sediment or rock.

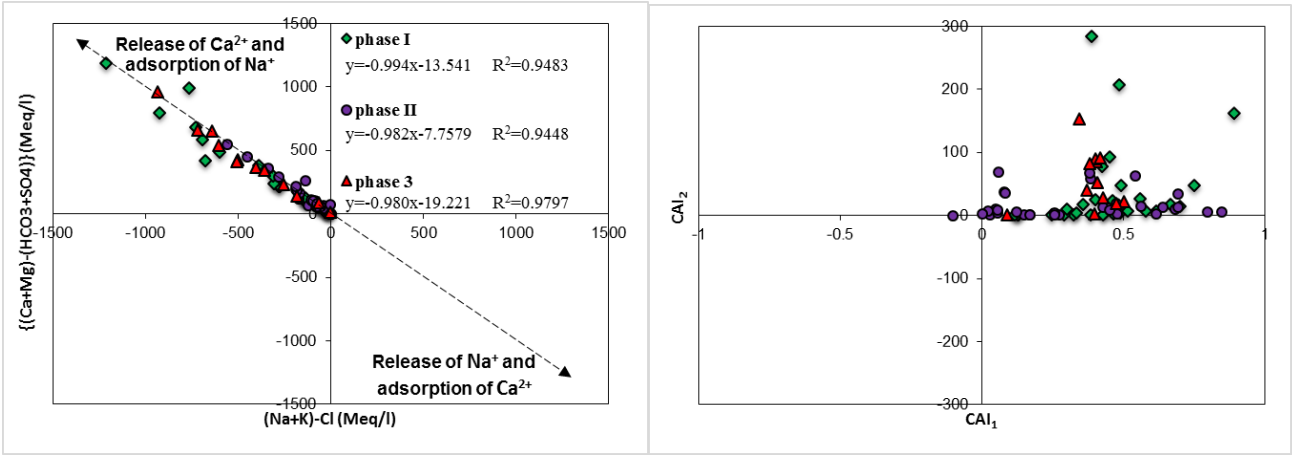

Fig. 10 $(Na^+ + K^+ - Cl^-)$ vs $(Ca^{2+} + Mg^{2+}) - (HCO_3^- + SO_4^{2-})$ and CAI-1vs CAI-2 Bivariate Graphs of mine groundwater samples

The graphs provided in this section collectively suggest that salinization, evaporation, and mineral crystallization play a significant role in the hydrochemical composition of groundwater in the area. Salinity mechanisms intensify at greater depths, as evidenced by the notably higher mean EC value in deep samples. Variations in the chemical composition of samples between wet and dry seasons imply potential scenarios involving evaporite dissolution and water mixing from different sources. The precise source of high salinity observed in the groundwater of this area remains uncertain, with hypotheses including the dissolution of evaporite minerals in the mining area, the dissolution of evaporite minerals in the Salt Lake, and subsequent hydraulic connections between the Salt Lake and the aquifers, or possibly a combination of these options. Nevertheless, the hydraulic connection between the aquifers and Salt Lake is largely rejected by the Br/Cl vs. B/Cl diagram. Further comprehensive investigations are required for this hypothesis, as will be discussed in the next section. In addition, diagrams 9 and 10 elucidate the significant influence of ion exchange, especially reverse softening, on the chemical composition of groundwater due to the presence of clay and silt interlayers in the alluvial aquifer.

Hydraulic connection between Kheirabad Salt Lake and mine area aquifers

Aquifers in the mining area and Kheirabad Salt Lake may be hydraulically linked via alluvial deposits and/or the Kheirabad fault, which is a potential source of groundwater in the mining area (Fig. 1). The

alluvium deposits exhibit low hydraulic conductivity. Moreover, the water table is higher in the northern part of the pit compared to the lake bottom. Consequently, it is not practical to flow water from the lake to the aquifers via the alluvial deposits. Nevertheless, a plausible scenario involves water movement from Salt Lake through the Kheirabad fault. Various geochemical plots and ratios are employed to assess the possible flow through the two mentioned pathways. To identify the origin of contamination and understand the mixing mechanisms, the Cl/Br and Cl/B mass ratios in groundwater samples can be utilized, as suggested by previous studies (Katz et al. 2011; Ettayfi et al. 2012). As presented in Fig. 11 and Fig. 12, groundwater samples exhibit no increase in Cl/B and Cl/Br ratios despite high Cl content (especially in samples of S19, S21, and 3242G-B). This finding suggests that there is no hydraulic connection between the mine aquifers and Kheirabad Lake.

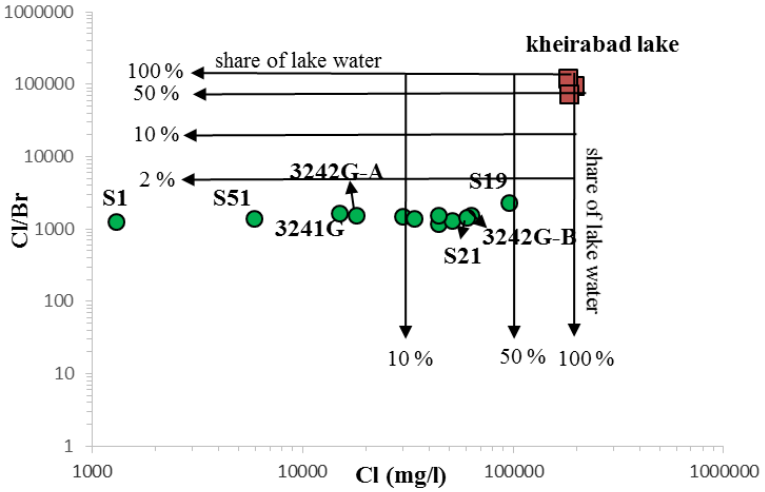

Fig. 11 Relationship of Cl/Br and chloride content in the samples, as compared to those from saltwater lake

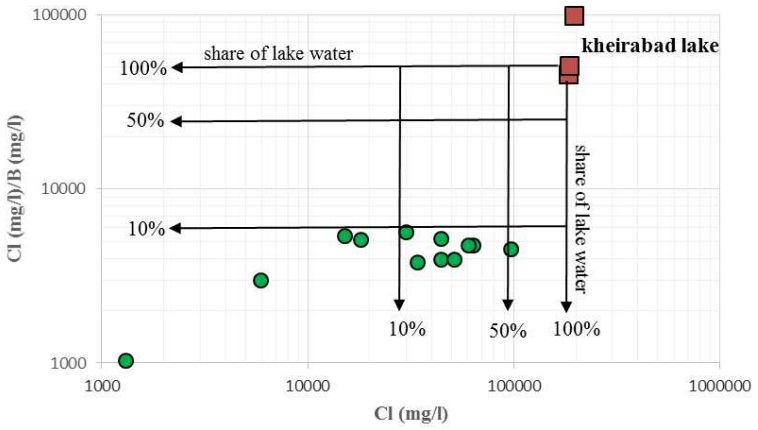

Fig. 12 Relationship of Cl/B and chloride content in the samples, as compared to those from saltwater lake

The Carpenter function (CF), which was identified by Knauth (1988) and derived from Carpenter's (1978) work, is the number of divalent cations that are exclusively balanced in charge by chloride ions. The equation for CF can be expressed as:

$$CF = Sr^{2+} + Mg^{2+} + Ca^{2+} - HCO_3^{-} - SO_4^{2-} \text{ (meq } L^{-1})$$

Several physicochemical mechanisms, including dolomitization, recrystallization, sulfate reduction, and precipitation or dissolution of minerals like calcite (CaCO3), gypsum (CaSO4), and salt, may lead to variations in ion concentrations; however, CF remains unaffected by these mechanisms (Chen et al. 2014).

The relationship between Br concentration and CF, as observed in the groundwater samples from the mining area, is presented in Fig. 13, which does not exhibit correspondence with the Kheirabad Salt Lake. Consequently, based on all conservative ions and ratios, it can be concluded that the groundwater in the Goharzamin pit area and the pit seepages do not originate from the Kheirabad Salt Lake.

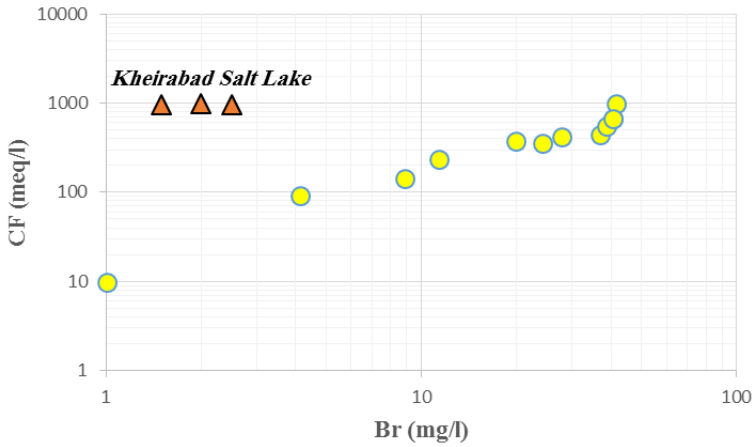

Fig. 13 Plot of CF versus Br concentration of groundwater and salt water lake samples

Isotope analysis and recharge conditions

Stable isotopes of oxygen ($\delta^{18}O$) and hydrogen ($\delta^{2}H$) are frequently employed in the study of the natural water cycle and groundwater flow as indicators for exploring the origin of groundwater and recharge mechanisms (e.g., Stefánsson et al. 2019; Carucci et al. 2012). These tracers have been studied to gain a deeper insight into the primary sources of the discovered ions and the different mechanisms that influence their contents in a specific area. Table 7 displays the isotopic composition of water samples that were collected during phase III. Also, in Fig. 14, the relationship between $\delta^{2}H$ and $\delta^{18}O$ for mine groundwater samples and Kheirabad Salt Lake samples (from Heidari-Nejad et al. 2017) is shown. In the diagram (Fig. 14), the Global Meteoric Water Line (GMWL) by the equation of $\delta^{2}H = 8\delta^{18}O + 10$ (Craig 1961), the East Mediterranean Meteoric Water Line (MMWL) by the relationship of $\delta^{2}H = 8\delta^{18}O + 22$ (Gat and Carmi 1970), the Iranian Meteoric Water Line (IMWL) by the linear equation of $\delta^{2}H = 6.89\delta^{18}O + 6.57$ (Shamsi and Kazemi 2014), and the Local Meteoric Water Line (LMWL) by the equation of $\delta^{2}H = 7.12\delta^{18}O + 15.92$ (Jahanshahi and Zare 2017) are also plotted. The IMWL and LMWL exhibit lower vapor humidity compared to the GMWL due to their lower slope values. The slope can be affected by several factors, including humidity, temperature, and other parameters (Gat and Gonfiantini 1981; Rozanski et al. 1997) that are unique to a certain groundwater medium.

As illustrated by Fig. 14, the samples stand near and to the bottom right of the GMWL and IMWL. This diagram also reveals that the majority of the samples lie along an evaporation line and enrichment process defined by equation: $\delta^{2}H = 5.4437\delta^{18}O - 13.78$. The samples exhibit a notable $\delta^{18}O$ enrichment with respect to meteoric water lines. The relatively low slope (5.44) and y-intercept (-13.78‰) observed in the mining area samples indicate the possibility of water evaporation either prior to or during water replenishment or the occurrence of significant rock-water interaction in the porous media (Banner et al. 1989; Al-Katheeri et al. 2009). The observed trend also might be created due to evaporation mechanisms occurring in fine-grained soils under arid conditions. (Sonntag et al. 1985; Gil-Márquez et al. 2016). The groundwater's composition would have been significantly enriched due to evaporation, caused by the water's gradual infiltration or seepage through the mine alluvium aquifer's fine clayey sands.

The samples of 3241G (groundwater) and Kheirabad Salt Lake exhibit a higher abundance of heavy isotopes in comparison to the others. The maximum $\delta^{18}O$-$\delta^{2}H$ values in these samples are 13.20-29.70‰ and 9.51-40.74‰, respectively. They had undergone intensive evaporation. The samples of surface water collected from Kheirabad Salt Lake exhibit an enrichment in the isotopes ^{18}O and ^{2}H, a characteristic sign

of evaporation in an exposed water body with low relative humidity in a continental arid and semi-arid climate (Clark and Fritz 1997). Infiltration of evaporated groundwater and surface water pumped from the mine pit and maintained at a pool near the 3241G borehole may explain the isotopic enrichment of groundwater sample 3241G in the south of Goharzamin mine. However, except for the sample of 3241G, the values of $\delta^{18}O$ and $\delta^{2}H$ of the area groundwater samples ranged from -5.74 to -2.5‰ and -37.8 to -27.78‰, respectively. The relationship between the $\delta^{2}H$ and $\delta^{18}O$ values in these samples can be described by the following least squares regression equation: $\delta^{2}H = 1.7511\delta^{18}O - 28.039$. An interaction between the porous medium and heated water, caused by deep groundwater circulation, is probably responsible for the observed slope.

Table 7 Isotopic composition of water samples in phase III

sample ID	$\delta^{18}O$ (‰ VSMOW)	$\delta^{2}H$ (‰ VSMOW)	^{3}H (TU)	$\delta^{13}C$ (‰ PDB)	^{14}C (pmC)
3242G-A	-4.80	-35.07	<0.8		
3242G-B	-2.89	-32.68	<0.8		
3313	-2.50	-27.78		-22.2	46.35
S10	-4.08	-36.18		-8.94	3.310
S19	-2.67	-35.86		-8.87	3.267
S3252	-3.49	-35.74	<0.8		
S51	-4.74	-36.00		-2.00	9.955
S1	-5.74	-37.80	<0.8		
3245	-3.69	-35.10			
S21	-3.23	-34.30			
SB-14	-3.92	-34.98		-11.50	11.43
3241G	9.51	40.74	5.2		
Lake	13.20	29.70			

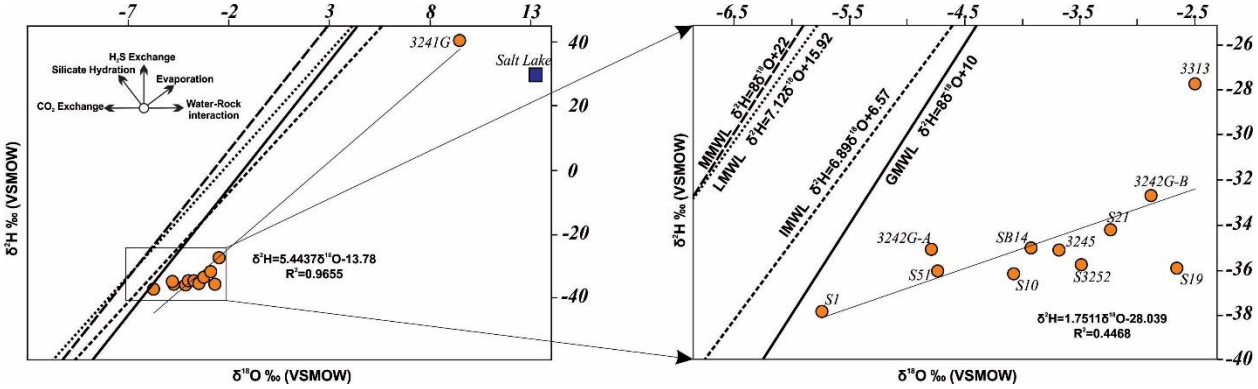

Fig. 14 Range of $\delta^{2}H$ and $\delta^{18}O$ in the Goharzamin pit samples in comarison to GMWL, MMWL, IMWL, and LMWL

The relationships between d-excess and $\delta^{18}O$ in all of the samples are illustrated in Figure 15. The d-excess, an index denoting the influence of evaporation on the physical and chemical characteristics of groundwater, is calculated as follows: $d = \delta^{2}H - 8\ \delta^{18}O$ (Dansgaard 1964). While the groundwater evaporates, the d-excess decreases; this process is independent of the basic isotopic composition of the starting water. The typical d-excess value on a global level is approximately 10‰; however, it varies depending on factors such as humidity, wind speed, and sea surface temperature during evaporation. Consequently, the low d-excess values indicate that there was a high level of humidity when the vapor mass was formed (Clarks and Fritz 1997). If the value of d-excess falls within the range of +5‰ (Carol et al. 2009) and +10‰ (Han et al. 2009), it indicates that the groundwater has evaporated prior to infiltration. This phenomenon is commonly observed in groundwater samples collected from arid and semi-arid regions. In general, a negative correlation between $\delta^{18}O$ and d-excess is typically observed in the samples collected from the studied area. The d-excess values of the groundwater samples (except for 3241G) vary from -14.54 to 8.09‰, with an average of -4.33‰. The study area exhibits a high level of

humidity due to the influence of both local and regional moisture circulation, as reflected by these ranges of values. The greater $\delta^{18}O$ and $\delta^{2}H$ values enrichments with depth (Fig. 16) probably indicate the warm climate of the area in the past.

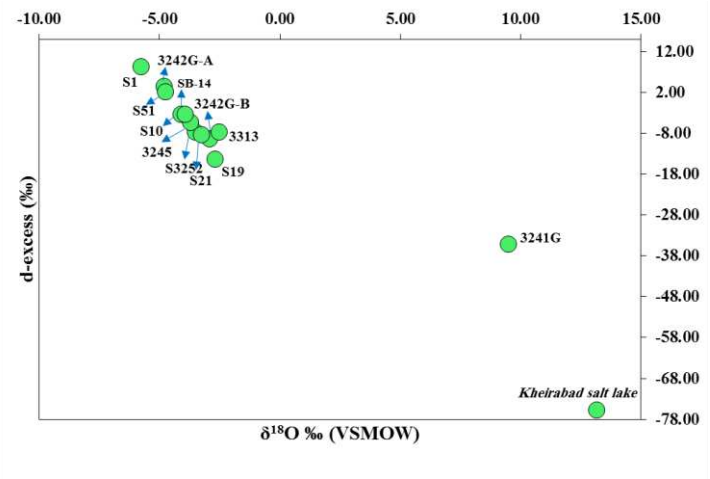

Fig. 15 The d-excess vs. $\delta^{18}O$ relationship

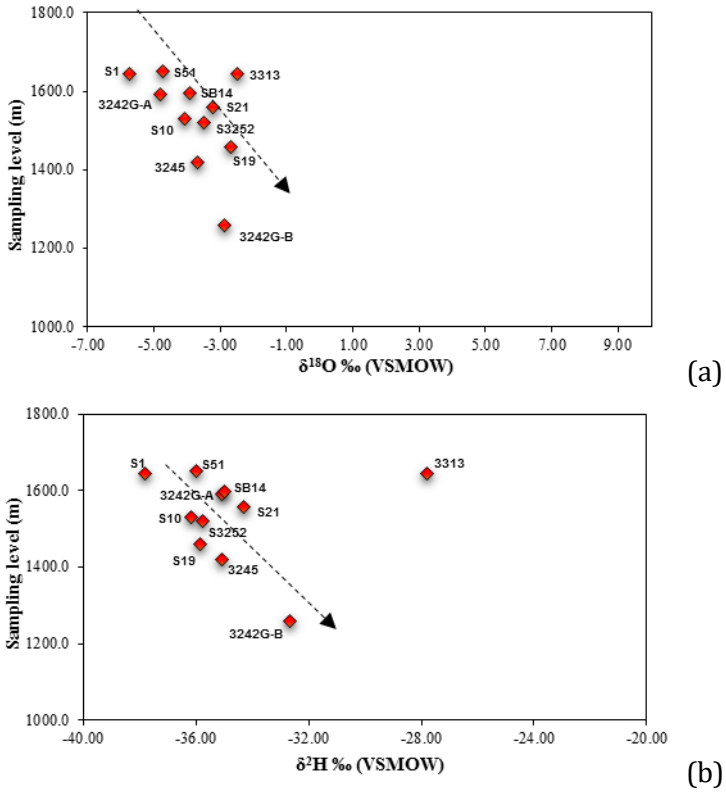

Fig. 16 The relationship of sampling level of the analyzed groundwater samples versus (a) $\delta^{18}O$ and (b) $\delta^{2}H$

The relation between salinity (or chloride) and $\delta^{18}O$ may be applied to determine the processes that lead to mineralization in groundwater, such as dissolution, evaporation, and saltwater intrusion. When examining the relationship between Cl content and $\delta^{18}O$ (as shown in Figure 17), it is observed that the samples demonstrate an increase in salinity within a limited range of $\delta^{18}O$ values. This would imply that the oxygen isotopes undergo changes as a result of the exchange reactions that take place between porous medium and water for a long time.

The relationship between chemical and isotopic data implies that evaporation and evaporite dissolution processes predominantly control the salinity of the mining area groundwaters, indicating that Kheirabad Salt Lake does not play a significant role in this phenomenon.

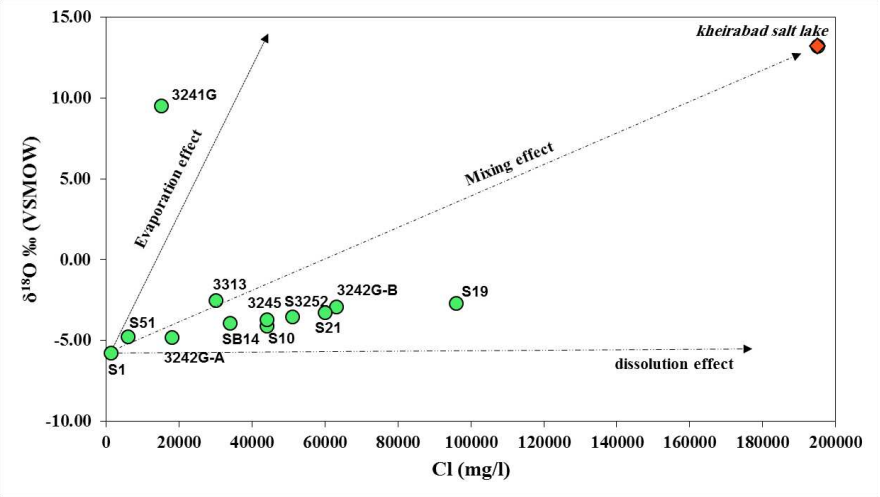

Fig. 17 Relationship between Cl content (in mg/L) and $\delta^{18}O$ (‰ VSMOW) of mine groundwater samples and salt lake

Groundwater dating or residence time

An analysis was conducted on the samples to determine the apparent residence time of groundwater in the Goharzamin mine area by measuring the carbon isotopes (^{14}C and $\delta^{13}C$) of dissolved inorganic carbon (DIC, primarily HCO_3^-) and tritium activities (3H). Tritium's short half-life of 12.4 years makes it beneficial for differentiating groundwater recharge before the nuclear bomb testing from water that is younger (<67 years ago), while Carbon-14 can be utilized for older groundwater systems because of its longer half-life of 5,730 years. Five samples were analyzed for each tritium and radiocarbon concentration. Most of the water samples were selected from deep basins, and they are not a good indicator of the whole mining area. However, the results of these analyzed samples could enhance our understanding of the hydrogeological system of the area. The tritium contents in the samples collected from the mine vary from below the detection limit (0.8) to 5.2 TU, as shown in Table 7. A high value (5.2 TU) is observed in the groundwater sample of 3241G, signifying a substantial contribution of modern precipitation and indicating recent water (< 10 years old). As previously mentioned, the groundwater sample of 3241G seems to indicate a mixing of surface water and groundwater. Among the five evaluated samples, four exhibit negligible tritium contents, below 0.8 TU. The findings imply that the groundwater in most boreholes and seepages was predominantly replenished by rainfall before 1952. In other words, the undetected ^3H concentrations reflect the long residence times of the water recharge (> 67 years, before 1952) through the aquifer, or they can be regarded as a binary mixture of older (pre-1952) and younger (post-1952) water. The delay in water penetration in the unsaturated zone and the expansion in groundwater residence time are caused by the high depth and low transmissivity of the clayey layers, which are interbedded with sandstones.

The radiocarbon (^{14}C) concentration and ^{13}C content of the analyzed samples range from 3.214 to 46.22 pmC and from -2 to -22.159‰, respectively (Table 7). The main problem with ^{14}C groundwater dating is often overestimations of groundwater ages (Jasechko 2016). When soil organic matter decomposes along flow paths or when carbonates dissolve, dead carbon is introduced into the system. This can significantly dilute the ^{14}C content and raise the apparent ^{14}C ages (Geyh 2000; Clark and Fritz 1997). Therefore, numerous methods for ^{14}C groundwater age correction (Ingerson and Pearson 1964; Evans et al. 1979; Eichinger 1983; Salem et al. 1980; Fontes and Garnier 1979; Tamers 1975) have been developed. Because of the possibility of dead carbon from carbonate-rich units, like the carbonate formation (Fig. 1), in places with hydraulic connections, using uncorrected radiocarbon ages in the groundwater system can be problematic. In this study, several correction methods using measured hydrochemical and isotopic

variables (alkalinity, pH, T, and $\delta^{13}C$ values) were employed to convert the measured ^{14}C content (in pmC) into groundwater ages (in yr). Based on various correction techniques and ^{14}C activity, the computed mean residence time of recharge indicates an age range of 6000 years (in the Holocene) to 29000 years (paleowater, in the late Pleistocene) (Table 8). In more detail, the groundwater age dating results in the identification of four distinct age categories. The first category consists of young waters resulting from recent precipitations such as surface water, runoff, and shallow subsurface discharge. The second category includes waters found in upper alluvial aquifer aged between 5000 and 8000 years, particularly during the Northgrippian ages in the middle of the Holocene epoch. In the third category, the groundwaters, especially in the lower section of the alluvial aquifer, fall between 12,000 and 19,000 years old, ranging from the Late Pleistocene to the early Holocene. Lastly, the fourth category comprises waters in hard rock aquifer exceeding 20,000 years but less than 30,000 years old, originating from the late Pleistocene epoch. An increase in age with depth can be observed in ^{14}C-analyzed samples (Fig. 18). Findings from the ^{14}C dating are in agreement with the ^{3}H concentration (dating) and the study by Gharaat et al. (2022).

These findings demonstrated that the deep groundwater that is currently seeping into the mine pit was not created by modern precipitation. However, chemical variations of the groundwater samples (seepages) in the rainy season in comparison to the dry season showed that new meteoric water was mixed with deep groundwater after surface evaporite dissolution and passing through the fractures around the mine pit.

Table 8 Computed age and isotopic variables of the ^{14}C analyzed Goharzamin samples

Sample	^{18}O (‰ vs. V-SMOW)	^{2}H (‰ vs. V-SMOW)	^{13}C (‰ vs. PDB)	^{14}C (pmC)	^{14}C-ERR	Age (pearson) (years)	Age (Evans) (years)	Age (Eichinger) (years)	Age (IAEA) (years)	Age (Fontes & Garnier (years)	Age (Tamers) (years)	Age brut A_0=100
S10	-4.08	-36.18	-8.94	3.257	0.055	20923	20519	22987	24449	20844	23025	28308
S19	-2.67	-35.86	-8.87	3.214	0.052	20973	20564	23491	24499	20846	24124	28419
S51	-4.74	-36.00	-2.00	9.725	0.076	-	-	-	-	-	14535	19265
3313	-2.50	-27.78	-22.2	46.22	0.22	6083	6073	3983	9609	7813	1326	6380
SB-14	-3.92	-34.98	-11.50	11.28	0.10	12582	12323	13799	16108	12569	12988	18042

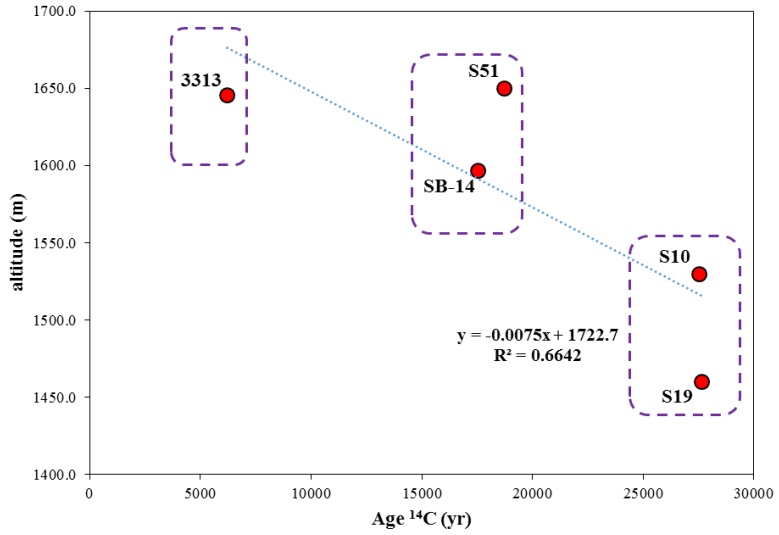

Fig. 18 The relationship of ^{14}C age versus altitude of the analyzed groundwater samples

Conclusions

This research employed a combination of hydrogeochemical indicators, stable isotopes, and statistical investigations to analyze the source of groundwater in the Goharzamin mine region as a multi-layered aquifer system (including hardrock and alluvial aquifers). In summary, the key findings can be stated as follows:

Groundwater in the Goharzamin mining area is generally saline or brine water, with an average of EC values equal to 48.39 to 58.57 mS cm^{-1} in the dry and wet seasons, respectively. The hydrochemical facies and water types are mainly Na-Cl, indicating long groundwater residence time and movement and/or relatively higher rock-water interaction. The dominant anion is Cl^-, followed by SO_4^{2-}, $HCO_3^-$and NO_3^-, while the dominant cation is Na^+, followed by Ca^{2+}, Mg^{2+} and K^+.

The two water groups obtained by the multivariate statistical analysis methods (PCA and HCA) could be globally discussed as two water types, indicating that similar geochemical mechanisms influence the hydro-geochemical constitution in the samples held by the same class. The first one is characterized by lower salinity and involves groundwater mainly located in the alluvium layer. The second water type has high salinity, observed mainly in the deep crystalline formation aquifer. This shows that the chemical mechanisms that affect the chemical composition of groundwater in the samples belonging to the same group are similar.

Geogenic (natural) factors, mainly including evaporite dissolution, mineral crystallization, reverse ion exchange, and rock-water interaction, play a pivotal role in the hydrogeochemical evolution of groundwater in the area.

The hydrochemical and isotopic interpretation shows that Kheirabad Salt Playa (about 13000 m in the north of the pit) could not be a significant source of groundwater in the mine area. Radiocarbon (^{14}C) corrected age and ^3H age dating confirm the presence of old groundwater, especially at deep aquifers, that was recharged during the Holocene and Late Pleistocene.

Finally, it has been confirmed that there are a minimum of three distinct aquifers in this complex multi-layered system. The variations in the groundwater chemical composition during the wet and dry seasons indicate that these aquifers are not completely isolated. These variations can be attributed to two factors. Firstly, the hydraulic connection that exists among the aquifers in certain areas, including faults and fractures around the mining area, Secondly, the significant hydraulic gradient produced by the pit excavation.

References

Abdrabo KI, Kantoush SA, Esmaiel A, Saber M, Sumi T, Almamari M, Elboshy B, Ghoniem S (2023) An integrated indicator-based approach for constructing an urban flood vulnerability index as an urban decision-making tool using the PCA and AHP techniques: A case study of Alexandria, Egypt. Urban Clim 48:101426. https://doi.org/10.1016/j.uclim.2023.101426

Acikel S, Ekmekci M (2021) Distinction of multiple groundwater systems in a coastal karst spring zone in SW Turkey by hydrochemical and isotopic characteristics. Bull Eng Geol Environ 80(7): 5781–5795. https://doi.org/10.1007/s10064-021-02150-4

Aduojo AA, Mosobalaje OO, Uchegbulam O, Johnson AO, Ifeanyi O (2024) Multivariate analysis of seasonal changes of chemical elements in groundwater around Solous lll dumpsite, Lagos, South-West Nigeria. Sci Afr 23: e02084. https://doi.org/10.1016/j.sciaf.2024.e02084

Al-Katheeri ES, Howari FM, Murad AA (2009) Hydrogeochemistry and pollution assessment of quaternary–tertiary aquifer in the Liwa area, United Arab Emirates. Environ Earth Sci 59: 581–592. https://doi.org/10.1007/s12665-009-0056-y

APHA-AWWA-WPCF (2005) Standard Methods for the Examination of Water and Wastewater. 21st Edition, American Water Works Association and Water Pollution Control Federation, Washington DC

Assari A (2019) Defining hydrogeology of the Gohar-Zamin open pit mine, Iran: a case study in a hard-rock aquifer. Hydrogeol J 27, 1479–1495. https://doi.org/10.1007/s10040-018-01919-4

Ayari J, Ouelhazi H, Charef A, Barhoumi A (2023) Delineation of seawater intrusion and groundwater quality assessment in coastal aquifers: The Korba coastal aquifer (Northeastern Tunisia). Mar Pollut Bull 188: 114643. https://doi.org/10.1016/j.marpolbul.2023.114643

Back W (1966) Hydrochemical facies and groundwater flow patterns in northern part of Atlantic Coastal Plain. US Geol Surv Prof Pap 498-A. https://doi.org/10.3133/pp498A

Banner JL, Wasseerburg GJ, Dobson PF, Carpenter AB, Moore CH (1989) Isotopic and trace-element constraints on the origin and evolution of saline groundwaters from central Missouri. Geochim Cosmochim Acta 53 (2):383–398. https://doi.org/10.1016/0016-7037(89)90390-6

Barbieri M, Boschetti T, Petitta M, Tallini M (2005) Stable isotope (2H, 18O and 87Sr/86Sr) and hydrochemistry monitoring for groundwater hydrodynamics analysis in a karst aquifer (Gran Sasso, Central Italy). J Appl Geochem 20 (11): 2063–2081. https://doi.org/10.1016/j.apgeochem.2005.07.008

Bhatt AG, Kumar A, Trivedi PR (2021) Integration of multivariate statistics and water quality indices to evaluate groundwater quality and its suitability in middle Gangetic floodplain, Bihar. SN Appl Sci 3:426. https://doi.org/10.1007/s42452-021-04394-x

Boumaiza L, Ben Ammar S, Chesnaux R, Stotler RL, Mayer B, Huneau F, Johannesson KH, Levison J, Knöller K, Stumpp C (2023) Nitrate sources and transformation processes in groundwater of a coastal area experiencing various environmental stressors. J Environ Manag 345:118803. https://doi.org/10.1016/j.jenvman.2023.118803

Carol E, Kruse E, Mas-Pla J (2009) Hydrochemical and isotopical evidence of ground water salinization processes on the coastal plain of Samborombón Bay, Argentina. J Hydrol 365 (3-4): 335-345. https://doi.org/10.1016/j.jhydrol.2008.11.041

Carpenter AB (1978) Origin and chemical evolution of brines in sedimentary basins. Oklahoma Geological Survey Circulars 79:60–77. https://doi.org/10.2118/7504-MS

Carucci V, Petitta M, Aravena R (2012) Interaction between shallow and deep aquifers in the Tivoli Plain (Central Italy) enhanced by groundwater extraction: A multi-isotope approach and geochemical modeling. J Appl Geochem 27(1):266-280. https://doi.org/10.1016/j.apgeochem.2011.11.007

Chai Y, Xiao C, Li M, Liang X (2020) Hydrogeochemical Characteristics and Groundwater Quality Evaluation Based on Multivariate Statistical Analysis. Water J 12:2792. https://doi.org/10.3390/w12102792

Chen L, Ma T, Du Y, Yang J, Liu L, Shan H, Liu C, Cai H (2014) Origin and evolution of formation water in North China Plain based on hydrochemistry and stable isotopes (2H, 18O, 37Cl and 81Br). J Geochem Explor 145:250–259. https://doi.org/10.1016/j.gexplo.2014.07.006

Clark ID, Fritz P (1997) Environmental Isotopes in Hydrology, Lewis Publishers, Boca Raton, USA

Craig H (1961) Isotopic variation in meteoric waters. sci 133(3465):1702-1703. doi: 10.1126/science.133.3465.1702

Dansgaard W (1964) Stable isotopes in precipitation. Tellus, 16:436–438. https://doi.org/10.1111/j.2153-3490.1964.tb00181.x

Dhurandhar AP, Ranjan R (2020) Imaging and integration of hydrogeochemical data for characterization of groundwater quality around Jabalpur, India. Bull Eng Geol Environ 79:109–131. https://doi.org/10.1007/s10064-019-01555-6

Eichinger E (1983) A contribution to the interpretation of 14C groundwater ages considering the example of a partially confined sandstone aquifer. Radiocarbon 25:347 – 356. https://doi.org/10.1017/S0033822200005634

Ettayfi N, Bouchaou L, Michelot JL, Tagma T, Warner N, Boutaleb S, Massault M, Lgourna Z, Vengosh A (2012) Geochemical and isotopic (oxygen, hydrogen, carbon, strontium) constraints for the origin, salinity, and residence time of groundwater from a carbonate aquifer in the Western Anti-Atlas Mountains, Morocco. J Hydrol 438-439:97-111. https://doi.org/10.1016/j.jhydrol.2012.03.003

Evans GV, Otler RL, Downing A, Monkhouse RA, Rae G (1979) Some problems in the interpretation of isotope measurements in United-Kingdom aquifers. Isotope Hydrology II, IAEA, Vienna, 639-708

Fabryka-Martin J, Whittemore DO, Davis SN, Kubik PW, Sharma P (1991) Geochemistry of halogens in the Milk River aquifer, Alberta, Canada. J Appl Geochem 6 (4):447–464. https://doi.org/10.1016/0883-2927(91)90044-P

Fang SC (2019) Study on 14C dating analysis of deep groundwater resources on islands. J Environ Radioact 208-209:105994. https://doi.org/10.1016/j.jenvrad.2019.105994

Farid I, Zouari K, Abid K, Ayachi M (2012) Hydrogeochemical investigation of surface and groundwater composition in an irrigated land in central Tunisia. J Afr Earth Sci 78:16-27. https://doi.org/10.1016/j.jafrearsci.2012.10.001

Feisal NAS, Kamaludin NH, Sani MFA, Ahmad DKA, Ahmad MA, Razak NFA, Ibrahim TNBT (2023) Anthropogenic disturbance of aquatic biodiversity and water quality of an urban river in Penang, Malaysia. Water Sci Eng 16(3):234-242. https://doi.org/10.1016/j.wse.2023.01.003

Fontes JC, Garnier JM (1979) Determination of the initial activity of the total dissolved carbon: a review of the existing models and a new approach. Water Resour Res 12:399 – 413. https://doi.org/10.1029/WR015i002p00399

Gat JR, Carmi H (1970) Evolution of the isotopic composition of atmospheric waters in the Mediterranean Sea area. J Geophys Res 75:3039-3040. https://doi.org/10.1029/JC075i015p03039

Gat JR, Gonfiantini R (1981) Stable Isotope Hydrology, Deuterium and Oxygen -18 in the Water Cycle. IAEA. Tech. Rept. Series No. 210, 337pp

Geyh MA (2000) An overview of 14C analysis in the study of groundwater. Radiocarbon 42(1):99-114. https://doi.org/10.1017/S0033822200053078

Gibbs RJ (1970) Mechanisms controlling world water chemistry. Sci 17:1088–1090. doi: 10.1126/science.170.3962.1088

Gil-Márquez JM, Barberá JA, Andreo B, Mudarra M (2016) Hydrological and geochemical processes constraining groundwater salinity in wetland areas related to evaporitic (karst) systems. A case study from Southern Spain, J Hydrol 544:538-554. doi: http://dx.doi.org/10.1016/j.jhydrol.2016.11.062

Hamma B, Alodah A, Bouaicha F, Bekkouche MF, Barkat A, Hussein EE (2024) Hydrochemical assessment of groundwater using multivariate statistical methods and water quality indices (WQIs). Appl Water Sci 14: 33. https://doi.org/10.1007/s13201-023-02084-0

Han D, Liang X, Jin M, Currell MJ, Han Y, Song X (2009) Hydrogeochemical Indicators of Groundwater Flow Systems in the Yangwu River Alluvial Fan, Xinzhou Basin, Shanxi, China. J Environ Manag 44:243-255. https://doi.org/10.1007/s00267-009-9301-0

Heidari-Nejad H, Zarei M, Merkel BJ (2017) Evaluating the Origin of Seepage Water in the Golgohar Iron Mine, Iran. Mine Water Environ 36:583–596. https://doi.org/10.1007/s10230-017-0447-3

Helstrup T, Jørgensen N, Banoeng-Yakubo B (2007) Investigation of hydrochemical characteristics of groundwater from Cretaceous—Eocene limestone aquifer in southern Ghana and Togo using hierarchical cluster analysis. Hydrogeol J 15:977-989. https://doi.org/10.1007/s10040-007-0165-1

Ingerson E, Pearson FJ (1964) Estimation of age and rate of motion of groundwater by the 14C method. In: Recent researches in the fields of hydrosphere, atmosphere and nuclear geochemistry. Sugarawa Festival volume, Maruzen, Tokyo, 263-283

Jahanshahi R, Zare M (2017) Delineating the origin of groundwater in the golegohar mine area of iran using stable isotopes of 2H and 18O and hydrochemistry. Mine Water Environ, 36, 550-563. https://doi.org/10.1007/s10230-017-0444-6

Jasechko S (2016) Partitioning young and old groundwater with geochemical tracers. Chem Geol 427:35–42. https://doi.org/10.1016/j.chemgeo.2016.02.012

Ju Q, Hu Y, Liu Q, Chen K, Zhang H, Wu Y (2024) Multiple stable isotopes and geochemical approaches to elucidate groundwater reactive transport paths in mining cities: A case from the northern Anhui, China. Sci Total Environ 912:169706. https://doi.org/10.1016/j.scitotenv.2023.169706

Kaiser HF (1960) The application of electronic computers to factor analysis. Educ Psychol Meas 20:141-151. https://doi.org/10.1177/001316446002000116

Katz BG, Eberts SM, Kauffman LJ (2011) Using Cl/Br ratios and other indicators to assess potential impacts on groundwater quality from septic systems: A review and examples from principal aquifers in the United States. J Hydrol 397:151-166. https://doi.org/10.1016/j.jhydrol.2010.11.017

Knauth PL (1988) Origin and mixing history of brines: Palo Duro Basin, Texas, USA. J Appl Geochem 3(5):455–474. https://doi.org/10.1016/0883-2927(88)90019-4

Krimissa S, Michelot JL, Bouchaou L, Mudry J, Hsissou Y (2004) About the origin of chloride in groundwater from a coastal aquifer under semi-arid climate (Chtouka-Massa, Morocco). C R Geosci 336 (15):1363–1369. https://doi.org/10.1016/j.crte.2004.08.003

Li H, Gao D, Wu J, Zhao D, Zhang L (2021) Determination method of water gushing runoff zones in the open pit mining area. Bull Eng Geol Environ 80(5):3953–3971. https://doi.org/10.1007/s10064-021-02186-6

Liu Z, Feng S, Zhangsong A, Han Y, Cao R (2023) Long-term evolution of groundwater hydrochemistry and its influencing factors based on self-organizing map (SOM). Ecol Indic 154:110697. https://doi.org/10.1016/j.ecolind.2023.110697

Mohammed MAA, Eltijani A, Szabó NP et al (2023) Hydro-chemometrics of the Nubian Aquifer in Sudan: an integration of groundwater quality index, multivariate statistics, and human health risk assessment. Discov water 3:15. https://doi.org/10.1007/s43832-023-00039-9

Moloantoa KM, Khetsha ZP, van Heerden E, Castillo JC, Cason ED (2022) Nitrate Water Contamination from Industrial Activities and Complete Denitrification as a Remediation Option. Water J 14:799. https://doi.org/10.3390/w14050799

Mussa KR, Mjemah IC (2023) Using hydrogeochemical facies and signatures for groundwater characterization and evolution assessment in aquifers with contrasting climate and geology in Tanzania. Appl Water Sci 13:201. https://doi.org/10.1007/s13201-023-01977-4

Nayak A, Matta G, Uniyal DP (2023) Hydrochemical characterization of groundwater quality using chemometric analysis and water quality indices in the foothills of Himalayas. Environ Dev Sustain 25:14229-14260. https://doi.org/10.1007/s10668-022-02661-4

Okofo LB, Bedu-Addo K, Martienssen M (2022) Characterization of groundwater in the 'Tamnean' Plutonic Suite aquifers using hydrogeochemical and multivariate statistical evidence: a study in the Garu-Tempane District, Upper East Region of Ghana. Appl Water Sci 12:22. https://doi.org/10.1007/s13201-021-01559-2

Ophori DU, Toth J (1989) Pattern of ground water chemistry in Ross Creek basin, Alberta, Canada. Ground Water 27:20–26. https://doi.org/10.1111/j.1745-6584.1989.tb00003.x

Rahman A, Jahanara I, Jolly YN (2021) Assessment of physicochemical properties of water and their seasonal variation in an urban river in Bangladesh. Water Sci Eng 14(2):139-148. https://doi.org/10.1016/j.wse.2021.06.006

Rotiroti M, Sacchi E, Caschetto M, Zanotti C, Fumagalli L, Biasibetti M, Bonomi T, Leoni B (2023) Groundwater and surface water nitrate pollution in an intensively irrigated system: Sources, dynamics and adaptation to climate change. J Hydrol 623:129868. https://doi.org/10.1016/j.jhydrol.2023.129868

Rozanski K, Johnsen SJ, Schotterer U, Thompson LG (1997) Reconstruction of Past Climates from Stable Isotopes records of palaeo-precipitation preserved in continental archives. Hydrol Sci J 42:725 - 745. https://doi.org/10.1080/02626669709492069

Saberinasr A, Morsali M, Hashemnejad A, Hassanpour J (2019) Determining the origin of groundwater elements using hydrochemical data (case study: Kerman water conveyance tunnel). Environ Earth Sci 78:198. https://doi.org/10.1007/s12665-019-8182-7

Salem O, Visser JH, Dray M, Gonfiantini R (1980) Groundwater flow patterns in the western Libyan Arab Jamahiriya. In: Arid zone hydrogeology: investigations with isotope techniques. IAEA Vienna 165 – 179

Samtio MS, Daahar Hakro AAA, Jahangir TM, Mastoi AS, Lanjwani MF, Rajper RH, Lashari RA, Agheem MH, Noonari MW (2023) Impact of rock-water interaction on hydrogeochemical characteristics of groundwater: Using multivariate statistical, water quality index and irrigation indices of chachro sub-district, thar desert, sindh, Pakistan. Groundw Sustain Dev 20:100878. https://doi.org/10.1016/j.gsd.2022.100878

Schoeller H (1967) Qualitative evaluation of groundwater resources (in methods and techniques of groundwater investigation and development). Water resource Series, UNESCO, Paris, (33), 44-52

Shamsi A, Kazemi GA (2014) A review of research dealing with isotope hydrology in Iran and the first Iranian meteoric water line. GEOPE 4(1):73-86. doi: 10.22059/JGEOPE.2014.51193

Sidhu N, Kaur L, Rishi MS, Din SNU, Tewari K, Singh P (2024) Integrating multivariate hydrogeochemical analysis with human health risk assessment: An inverse geochemical and statistical modeling approach. J Geochem Explor 258:107389. https://doi.org/10.1016/j.gexplo.2024.107389

Sonntag C, Christmann D, Munnich KO (1985) Laboratory and field experiments on infiltration and evaporation of soil water by means of deuterium and oxygen-l 8. In: Stable and Radioactive Isotopes in the Study of the Unsaturated Zone, IAEA-TECDOC-357, IAEA Vienna, 145-160

Sophocleous M, Townsend MA, Whittemore DO (1990) Movement and fate of atrazine and bromide in central Kansas croplands. J Hydrol 115 (1–4):115–137. https://doi.org/10.1016/0022-1694(90)90201-8

Stefánsson A, Arnórsson S, Sveinbjörnsdóttir AE, Heinemaier J, Kristmannsdóttir H (2019) Isotope (δD, $\delta^{18}O$, ^{3}H, $\delta^{13}C$, ^{14}C) and chemical (B, Cl) Constrains on water origin, mixing, water-rock interaction and age of low-temperature geothermal water. J Appl Geochem 108: 104380. https://doi.org/10.1016/j.apgeochem.2019.104380

Subba Rao N, Sunitha B, Sun L, Deepthi Spandana B, Chaudhary M (2020) Mechanisms controlling groundwater chemistry and assessment of potential health risk: A case study from South India. Geochem 80(4):125568. https://doi.org/10.1016/j.chemer.2019.125568

Surinaidu L, Gurunadha Rao VVS, Srinivasa Rao N, Srinu S (2014) Hydrogeological and groundwater modeling studies to estimate the groundwater inflows into the coal Mines at different mine development stages using MODFLOW, Andhra Pradesh, India. Water Resour Ind 7–8:49-65. http://dx.doi.org/10.1016/j.wri.2014.10.002

Tamers MA (1975) Validity of radiocarbon dates on groundwater. Surv Geophys 2:217 – 239. https://doi.org/10.1007/BF01447909

Whittemore DO (1995) Geochemical differentiation of oil and gas brine from other saltwater sources contamination water resources: case studies from Kansas and Oklahoma. Environ Geosci 2(1): 15–31

Whittemore DO, Davis SN (1995) Patterns of Cl/Br with Cl concentration in the hydrosphere. Geological Society of America Abstracts with Programs 27(6):465–466

WHO (2006) Guidelines for drinking water quality, vol. 1, World Health Organisation, Geneva, Recommendations http://www.who.int/iris/handle/10665/42852

Wu Q, Mu W, Xing Y, Qian C, Shen J, Wang Y, Zhao D (2017) Source discrimination of mine water inrush using multiple methods: a case study from the Beiyangzhuang Mine, Northern China. Bull Eng Geol Environ 78:469-482. https://doi.org/10.1007/s10064-017-1194-1

Zhao X, Peng W, Chen K, Qiu X, Sun L (2022) Potential hydraulic connectivity of coal mine aquifers based on statistical analysis of hydrogeochemistry. Water Sci Eng 15(4):285-293. https://doi.org/10.1016/j.wse.2022.08.004

Zouari K, Trabelsi R, Chkir N (2011) Using geochemical indicators to investigate groundwater mixing and residence time in the aquifer system of Djeffara of Medenine (southeastern Tunisia). Hydrogeol J 19:209-219. https://doi.org/10.1007/s10040-010-0673-2